THESIS FOR THE DEGREE OF DOCTOR OF PHILOSOPHY

Using affordable iron oxide-based materials as oxygen carriers for biomass conversion

FELICIA ELIASSON STÖRNER

Department of Space, Earth and Environment

CHALMERS UNIVERSITY OF TECHNOLOGY

Gothenburg, Sweden 2024

Using affordable iron oxide-based materials as oxygen carriers for biomass conversion

FELICIA ELIASSON STÖRNER
ISBN 978-91-8103-122-5

Doktorsavhandling vid Chalmers tekniska högskola
Ny serie nr: 5580
ISSN 0346-718X

Department of Space, Earth and Environment
Chalmers University of Technology
SE-412 96 Gothenburg
Sweden
Telephone + 46 (0)31-772 1428

Cover: Elemental distribution of iron (Fe), silicon (Si), potassium (K), calcium (Ca), and phosphorous (P) in a cluster of copper slag particles. The particles have been subject to interaction with KH_2PO_4 which has resulted in agglomeration. The pictures are produced by SEM-EDS analysis

Printed by Chalmers Digital Print
Gothenburg, Sweden 2024

Abstract

Fluidized bed combustion is a mature technology that is well-established in the Swedish energy system. It is an especially suitable technology for conversion of biomass- and waste-derived fuels, which have high shares of volatiles and contain reactive ash species. Typically, silica sand is used as bed material, and it is inert with respect to the fuel conversion. However, recent developments have shown that fluidized bed combustion can be upgraded by utilizing oxygen carriers – bed materials that participate actively in the oxygen transport in the boiler. This concept is called Oxygen Carrier Aided Combustion (OCAC) and makes it possible to operate existing boilers at a reduced air-to-fuel ratio, increased efficiency, higher load, and potentially improved economic performance and reduced environmental impact.

OCAC makes use of oxygen carriers in the form of solid particles of transition metal-oxides. The material needs to be chemically active and have suitable fluidization properties, as well as sustained particle integrity at high temperatures and mechanical stress. The conversion of solid biomass- and waste-derived fuels is especially challenging because they are associated with corrosion, bed agglomeration, and slagging due to a high content of reactive ash species such as potassium. Fluidized bed combustion of such fuels necessitates a high rate of bed material replacement, so the material must be cheap and abundant. As a future step, oxygen carriers could be applied in a process known as Chemical-Looping Combustion (CLC), to produce undiluted CO_2 suitable for storage and utilization, but CLC has yet to be demonstrated on a commercial scale. OCAC could act as an intermediate step between conventional combustion and CLC, and potentially accelerate the implementation of large-scale carbon capture and storage necessary for meeting climate targets.

This thesis explores the possibilities for utilizing oxygen carrier materials that are already available in the Swedish metallurgical industries. Copper smelter slag was identified as a particularly suitable material due to its large production quantities, limited utilization and the low need of material processing required. Its properties were investigated, and its ability to absorb potassium without severe agglomeration was established by means of lab-scale interaction experiments with ash model compounds. Semi-commercial scale operation of a fluidized-bed boiler with copper smelter slag revealed suitable oxygen-carrying and fluidization properties, and good general performance.

Apart from these promising findings, a better understanding of potassium interactions with iron-based oxygen carriers in general was obtained by lab-scale experiments. Iron-oxides (iron mill scale and magnetite fines), iron-titanium-oxide (ilmenite), and two industrial slags (copper smelter slag and LD-slag) and their interaction with ash model compounds under different conditions were studied. The lab-scale studies included the development of a new method that allows for the addition of ash model compounds in connection to redox experiments at fluidized bed conditions. By comparing the results from different methods (fixed bed, fluidized bed, and large-scale boiler operation), it was concluded that the small-scale experiments are useful for an initial understanding of ash interaction. This is therefore a useful tool for estimating the risks of, for example, agglomeration before applying a new bed material in a full-scale boiler.

Acknowledgements

Thank you (YOU) for picking up this thesis to read. Maybe you're just getting started, maybe you're way ahead of me. Maybe you're just desperately looking for more references for your paper (I get it, I won't tell). Regardless, here we are – trying to understand what the hell is going on out there, maybe even contribute a little. Ok, let's get started.

My examiner Tobias Mattisson, thank you for challenging me to do better. K_2CO_3 decomposition won't get the best of us!

Magnus Rydén, who has supervised me through this. Thank you, for encouraging me to be creative and smart and helping me to focus on what's important.

Pavleta Knutsson, thank you for all your enthusiasm and for the warmth you bring to every meeting.

And thank you to Fredrik Lind, for providing me with direction and momentum when I started as a PhD student.

I want to acknowledge the Swedish Research Council (2017–04553), the Swedish Energy Agency (2022-00557), Boliden and E.ON. for funding this research.

There's been a lot of work going into writing the following pages. In the process, I have learned a lot, and I've had the pleasure of working with amazing people. There's so much more to say than what will fit on this page, but I'll give you a taste: ¶ In the lab I have learned about patience and Swagelok fittings (they come in millimetres AND inches! Both of them!). Rustan, Johannes, Jessica, Fredrik, Henrik, Victor, Ivana, Ivan, Robin, Viktor, Daofeng, and Tomas, thanks for all your support, your time, and your commitment. ¶ At the lunch table, I have learned about winemaking, Russian literature, windsurfing, music, solar panels, moon cakes, knitting patterns, dumplings, GVFÖ, and Zelda. ¶ I've met Karl and Simon and together we learned about the loudest sound in the world at an Aphex Twin concert. What an experience! ¶ In a parallel universe (Hops, Andra Långgatan) I've met new friends that have stayed with me though trivia and badminton. One of them even moved in with me! Very dedicated quiz team indeed. All of the people involved have helped making these past 5 years ~~bearable~~ enjoyable. Thank you!

Thank you also to all my friends out there for all the support and good vibes!

And finally, mamma pappa william julius, you're always there for me, thank you <3

Oh,

Look at me, still talking when there's science to do...

List of publications

Apart from the below mentioned contributions, Felicia is also the principal author of all five papers and is responsible for the writing and editing of the papers.

Paper I F. Störner, F. Hildor, H. Leion, M. Zevenhoven, L. Hupa, and M. Rydén, "Potassium Ash Interactions with Oxygen Carriers Steel Converter Slag and Iron Mill Scale in Chemical-Looping Combustion of Biomass - Experimental Evaluation Using Model Compounds," *Energy and Fuels*, vol. 34, no. 2, pp. 2304–2314, 2020, doi: 10.1021/acs.energyfuels.9b03616.

Contribution: Responsible for all the experimental work and data evaluation. Responsible for planning and preparing samples for the material analysis.

Paper II F. Störner, P. Knutsson, H. Leion, T. Mattisson, and M. Rydén, "An improved method for feeding ash model compounds to a bubbling fluidized bed – CLC experiments with ilmenite, methane, and K2CO3," *Greenh. Gases Sci. Technol.*, vol. 13, no. 4, pp. 546–564, 2023, doi: 10.1002/ghg.2218.

Contribution: Responsible for all the experimental work, including designing and testing the reactor, conducting the experiments, and data evaluation. Responsible also for all the material analysis, including planning, sample preparation, characterization and evaluation.

Paper III F. Störner, I. Staničić, P. Knutsson, T. Mattisson, and M. Rydén, "Potassium Interactions with Copper Slag and Magnetite Fines in Chemical-Looping Processes" *Submitted, under review*.

Contribution: Responsible for all the experimental work, including designing and testing the reactor, conducting the experiments, and data evaluation. Responsible also for all the material analysis, including planning, sample preparation, characterization and evaluation.

Paper IV F. Störner, F. Lind, and M. Rydén, "Oxygen Carrier Aided Combustion in Fluidized Bed Boilers in Sweden — Review and Future Outlook with Respect to Affordable Bed Materials," *Appl. Sci.*, vol. 11, no. 17, 2021, doi: https://doi.org/10.3390/app11177935.

Contribution: Responsible for the main part of the data collection and evaluation, and for planning the paper.

Paper V F. Störner, R. Faust, P. Knutsson, and M. Rydén, "Oxygen Carrier Aided Combustion with Copper Smelter Slag as Bed Material in a Semi-Commercial Wood-Fired Circulating Fluidized Bed" *Submitted*.

Contribution: Responsible for the main part of planning the experiments and planning the material analysis. Responsible for all the data evaluation.

Table of contents

List of abbreviations

BET (surface area) = Braunauer, Emmett and Teller (surface area)

BFB = Bubbling Fluidized Bed

BECCS = Bio-Energy Carbon Capture and Storage

CCS = Carbon Capture and Storage

CCUS = Carbon Capture Utilization and Storage

CFB = Circulating Fluidized Bed

CLC = Chemical-Looping Combustion

CLG = Chemical-Looping Gasification

CLOU = Chemical-Looping Oxygen Uncoupling

EDS = Energy-Dispersive X-ray Spectroscopy

FBC = Fluidized Bed Combustion

MAF = Magnetite Fines

MSW = Municipal Solid Waste

OCAC = Oxygen Carrier Aided Combustion

SEM = Scanning Electron Microscopy

TGA = Thermogravimetric Analysis

XRD = X-ray Diffraction

1. Introduction

Sweden has a long history of using domestic, renewable energy sources in the form of biomass- and solid waste-derived fuels. Many existing commercial boilers in Sweden today therefore use Fluidized bed combustion (FBC) technologies, as the complex nature of solid biomass and waste-derived fuels makes FBC a particularly useful combustion technology for these fuels. The fluidized bed has a high thermal inertia, allows for efficient mixing of air and fuel, and can absorb reactive ash species, among other advantages [1], [2], [3], [4]. There are currently around 120 FBC boilers in Sweden, about 1/3 of those are circulating fluidized beds (CFB) and the rest are bubbling fluidized beds (BFB) [5].

Conventional FBC applies a bed material that is inert with respect to the fuel conversion. Silica sand is the most common option – it can absorb ash species and be replaced at a high rate, as it is a low-cost material. Recently, the utilization of bed materials that are active in the fuel conversion process has been explored. Such materials are called oxygen carriers, and they can provide oxygen for the fuel conversion in addition to, or instead of, the gaseous oxygen fed by combustion air. Oxygen carriers can be used as bed material in FBC instead of an inert bed material, and thus, upgrade the process by making oxygen more available in the boiler [6]. This concept is called Oxygen Carrier Aided Combustion (OCAC). Furthermore, silica sand is a finite resource and sand reserves should be protected according to the Swedish environmental goals. This further motivates the utilization of alternative bed materials.

Using oxygen carriers in fluidized beds was first introduced for Chemical-Looping Combustion (CLC), which is a technique for producing pure CO_2 without energy-intensive gas separation. That the CO_2 stream is produced separately from the other flue gases makes CLC a suitable technology to combine with carbon capture and storage. Biomass-CLC could be a promising technique for Bio-Energy Carbon Capture and Storage (BECCS), which result in negative CO_2 emissions.

For a successful utilization of oxygen-carrying materials, it is important to consider the following aspects:

- Is the material reactive with fuel and air, i.e. is it an active oxygen carrier?
- The harsh conditions in the boiler with high temperatures and reactive ash species will likely require a high replacement rate of bed material. Is the lifetime of the material acceptable in relation to its cost?
- Is the material available in large quantities, and how much processing is required to produce a bed material from available products?

The reactivity with fuel and air can be demonstrated with quite simple methods. The two last points are less straightforward, as there are several parameters influencing, for example, the lifetime of the bed material in the boiler. The focus here has been on alkali interactions, as alkali from biomass and waste-derived fuels is expected to have major impact on the lifetime and performance of the oxygen carriers. The last point has been explored by discussing possible bed material production processes and comparing production quantities in available industries with the estimated demand.

1.1. Aim of the thesis and included papers

The overall aim of this thesis was to investigate possibilities and options for large-scale utilization of oxygen carriers for the conversion of biomass and waste-derived fuels. Much prior work has been done to develop new materials, but the focus of this thesis is on utilizing low-cost materials available in the metallurgical industry, such as slags and intermediate products, as oxygen carriers. These are seen as promising candidates for the given conditions due to both their properties and their large production quantities. More specifically, the work has focused on the following research objectives:

- Deepen the understanding of alkali interactions with oxygen carriers. The studied materials consisted of combinations of mainly Fe-, Si-, Ti-, and Ca-oxides. Oxygen carriers of almost pure Fe-oxide were compared with oxygen carriers with varying amounts of other oxides, and this helps understand the affinity of alkali towards different phases and for predicting which materials have a high risk of agglomeration.
- Develop a new experimental method that allows for simultaneous fluidization, fuel conversion, reduction, oxidation and alkali exposure of oxygen carriers, to study alkali interactions under conditions relevant for OCAC and CLC.
- Assess the fuel conversion and fluidization behavior of copper slag, magnetite fines and ilmenite in CLC cycles with the presence of potassium.
- Examine using a commercial copper smelter slag as oxygen-carrying bed material in an industrial-scale CFB boiler, focusing on general operability, emissions, and material ageing.

Paper I, II and **III** deal with alkali interactions on a more detailed level, using lab-scale experimental setups and pure alkali salts to simulate the contribution of alkali from the ash. These experiments have two main objectives (i) deepening the understanding of alkali interactions with relevant bed material components and drawing general conclusions to be applied when considering new, untested materials, (ii) making a first judgement regarding specific oxygen carriers, to decide if they are interesting to study further, specifically for the applications of high-alkali fuels. A new fluidized bed reactor was constructed and applied in **Paper II** and **III**, to account for the fluidization properties of the oxygen carriers. The findings from these studies are presented in section *4. Results Part I: Interactions with ash compounds*.

Paper IV had a somewhat different focus, where the utilization of oxygen carriers for OCAC and CLC was discussed from a broader perspective, taking into account practical considerations like material availability, transportation, procurement, and cost of oxygen carriers. Large-scale OCAC operation was reviewed, and different sources of potential low-cost oxygen carriers were discussed with a focus on Sweden and the Nordics. The findings from these studies are discussed in section *5. Results Part II: Large-scale OCAC operation*. Based on the lab scale investigation and the discussion presented in **Paper III** and **IV**, copper smelter slag was identified as a highly interesting alternative, based on its material properties and large production quantities. Copper smelter slag was therefore investigated as an oxygen carrier in an experimental campaign in a semi-industrial scale CFB boiler. Apart from studying the general operability and the oxygen carrying-properties of the material, the results were compared to the findings in the lab-scale fluidized bed reactor to evaluate the method. The findings from this study are presented in **Paper V**.

2. Theoretical background

2.1. Fluidized bed combustion of solid fuels

Solid fuels can be divided into four components: moisture, volatiles, char, and ash-forming matter [7]. As opposed to for example gaseous fuels, that burn directly in contact with heat and air, the conversion of solid fuels takes place in several steps. These are illustrated in Figure 1. When the fuel enters the boiler and heats up, it first dries, and the moisture is released as steam. The volatile fraction then evaporates quickly from the fuel. The volatiles contain hydrocarbons that are converted in contact with gaseous oxygen from the air. The remaining part of the fuel is the char. The char can be converted by direct char combustion in reaction with gaseous oxygen. The char conversion can also be via gasification, in which the char first reacts with CO_2 and H_2O, forming CO and H_2, which are then oxidized by gaseous oxygen. The final part of the fuel is the ash forming matter. The ash content and composition depend on the fuel, and the different ash species undergo transformations in the boiler, in which they might react with the bed material, react with other parts of the boiler equipment, or form small particles exiting as fly ash [8].

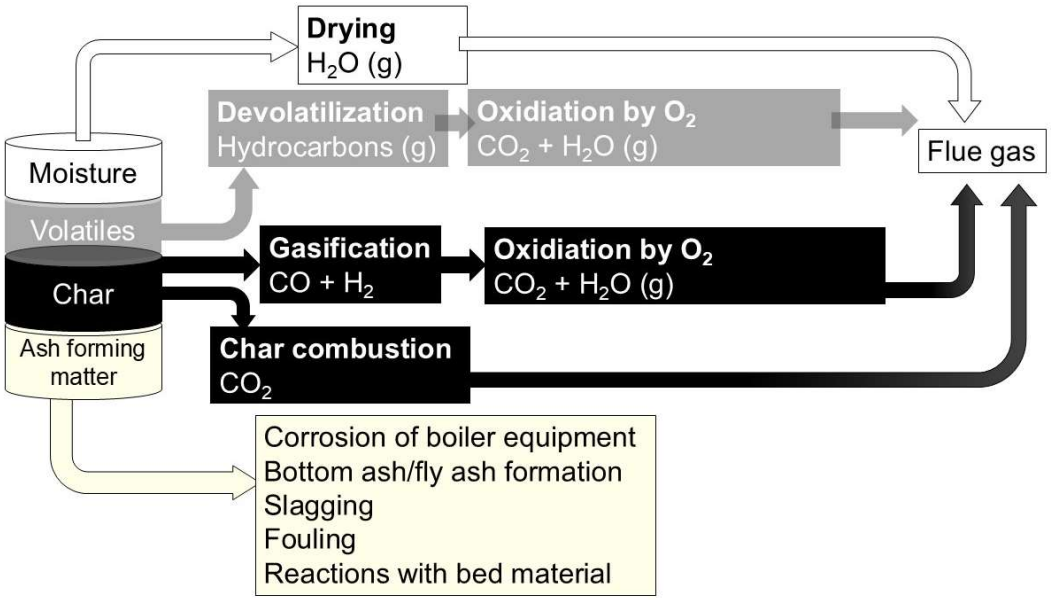

Figure 1: *Solid fuel conversion with gaseous oxygen.*

Different solid fuels have different distributions of the four fuel components, as well as different compositions within the volatiles, char, and ash fractions. FBC was originally developed for coal combustion [9]. As coal is still the most used solid fuel globally [10], it's important to point out some major differences between coal and solid biomass- and waste-derived fuels. In biomass and waste-derived fuels, typically [7], [9], [11], [12],

- The moisture and volatile contents are high
- The char is more reactive, i.e. gasification and char combustion are fast
- The total ash content is low in for example woody biomass, but on the other hand the ash contains alkali and other species that makes it very reactive, and

- The fuel composition (especially for waste-derived fuels) is inhomogeneous and can vary rapidly during feeding.

The ultimate analysis of wood (fir, spruce and pine), straw, municipal solid waste (MSW), and two types of coal (lignite and bituminous coal) are presented in Figure 2. The ash content in wood is low, and highest in MSW. Wood, straw, and MSW have high shares of moisture and volatiles, while the coals contain more fixed carbon (i.e. the carbon that remains in the char).

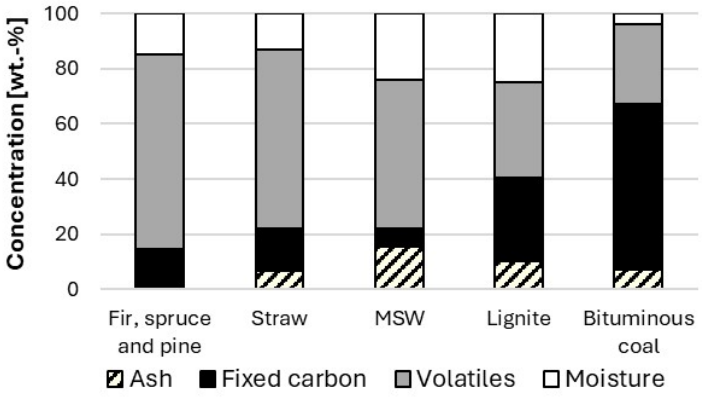

Figure 2: *Ultimate analysis of some fuels. The data is from Phyllis2, database for (treated) biomass, algae, feedstocks for biogas production and biochar, https://phyllis.nl/, TNO Biobased and Circular Technologies*

These aspects are important to consider when designing the fuel conversion process. The high content of volatiles in biomass and waste means that there might be dispersion problems in the boiler, since large amounts of volatiles are released close to the fuel feeding location. Further, the ability of the bed material to absorb certain ash species becomes important if the fuel contains species such as for example alkali. Ash interactions with bed material is one of the main topics of this thesis, and a more detailed background will be provided section 2.3.

Some of the advantages of fluidized beds are that [1], [2], [3], [4], [9], [13]

- **The bed material provides thermal inertia.** Sudden variation in the fuel composition can be expected with biomass and waste-derived fuels. The bed can provide stability with respect to temperature and heat transfer even during fluctuations in the fuel heating value.
- **The mixing between air and fuel is efficient.** The air-to-fuel ratio usually can be lower than in, for example, grate fired boiler, which is positive for the overall thermal efficiency of the boiler.
- **The bed material can absorb volatile ash species.** Especially the high alkali contents of biomass and waste-derived fuels can cause corrosion and other related problems in the boiler, but if it's absorbed by the bed, it won't have the same ability to cause such problems.
- **Relatively low temperature.** Typical bed temperatures in FBC are around 800-850°C. Thermal NOx-formation and severe high-temperature corrosion can be comparably low.
- **Fuel flexibility.** The boiler could be designed to being able to handle a variation of fuels.

2.2. Oxygen carriers and their properties in solid fuel conversion

Oxygen carriers consist of solid particles containing transition metal oxides that can switch between different oxidation states, depending on the surroundings. The main function of the oxygen carrier is to transport oxygen between different locations in the process and react with fuel and oxygen. The interaction with fuel is exemplified in Reaction (1), by the conversion of methane with a general metal oxide Me_xO_y. The reaction results in full oxidation of the methane and a reduction of the oxygen carrier.

$$Me_xO_y + CH_4 \rightarrow Me_xO_{y-4} + CO_2 + 2H_2O \qquad \text{Reaction (1)}$$

The reduced oxygen carrier subsequently reacts with oxygen in the air in another part of the process and becomes oxidized. This is generalized by Reaction (2)

$$Me_xO_{y-4} + 2O_2 \rightarrow Me_xO_y \qquad \text{Reaction (2)}$$

For CLC and OCAC to be viable, suitable oxygen carriers are required, preferably at a cost that is comparable to that of silica sand, which is the most used bed material in FBC of biomass and waste fuels. Materials should:

- **Be reactive with fuel and oxygen.** Both fuel conversion and re-oxidation of the oxygen carrier are crucial for the process, and the reactivity should be maintained over many cycles of reduction and oxidation.
- **Be durable.** During operation, the particles are exposed to mechanical stresses, high temperatures, and reactive ash compounds. Attrition and agglomeration must be at acceptable levels, as too short lifetimes of the material will not be economically feasible.
- **Be environmentally benign.** Both production and ash disposal should be considered.
- **Have good fluidization properties.** The fluidization depends on material properties such as particle size distribution, particle shape, and density.
- **Be economically feasible.** The acceptable cost per ton depends on the application and the expected lifetime of the material. For example, in MSW combustion, the lifetime is likely to be short due to the harsh environment and ash interactions.

Historically, the oxygen carriers studied the most are synthetic particles with oxides of Fe, Cu, Mn, and Ni [14], [15]. In many cases, pure metal oxides themselves have high reactivity but can't sustain good mechanical properties. Synthetic composite materials can be produced by combining the active metal oxide with some inert support material, which makes them more durable. This can produce very powerful materials in terms of fuel and oxygen reactivity. However, production is expensive, and very long lifetimes are likely required for them to be economically viable [16]. Thus, they are likely not suitable with biomass and waste-derived fuels, due to the harsh ash interactions [9], [11], [16]. Synthetic materials are not discussed further in this work.

The materials in focus here are instead low-cost, iron-based naturally occurring minerals or by-products from metallurgical industries. Iron oxide materials are abundant, have relatively low price and have shown good reactivity with both oxygen and fuel [16]. Due to their lower production cost compared to synthetic materials, a few hundred hours of residence time in the

boiler is likely sufficient for such materials [17]. Spent material could potentially become affordable raw material for downstream processes. Iron oxides have relatively high melting points, which enables a wide range of process temperatures [14], [18]. Due to their high melting point, Fe-oxides are not expected to suffer from agglomeration, in contrast to, for example, Cu-oxides. Fe-oxide itself is non-toxic [19], although other components in ore or by-product materials might be problematic. When used as an oxygen carrier, the most oxidized form of iron is hematite (Fe_2O_3, Fe^{3+}). During fuel conversion, hematite is reduced to magnetite (Fe_3O_4, $Fe^{3+,2+}$) and potentially further down to wüstite, (FeO, Fe^{2+}) or even elemental Fe. Reducing iron oxide beyond magnetite is, however, associated with an increased risk of agglomeration, as explained for example by Purnomo et al. [20], and Moldenhauer et al. [21].

One well-studied iron-based oxygen carrier is ilmenite, $FeTiO_3$, which is a titanium-iron oxide that is industrially mined and concentrated to produce TiO_2. Norwegian rock ilmenite and Australian sand ilmenite have been successfully used as bed materials in FBC and have properties in line with the requirements in the above-mentioned list. These activities have resulted in several publications, to which references can be found in Table 1. Ilmenite has also been subject to many CLC lab-scale experiments (many references can be found in [16]). The most oxidized form of ilmenite (the Fe^{3+}-phase) is Fe_2TiO_5 (pseudobrookite) and the Fe^{2+}-phase is $FeTiO_3$ (ilmenite). The other materials discussed in this thesis are based on by-products from the steel and copper industries, as well as ore concentrates

- **Copper smelter slag.** Copper smelter slag is a by-product of the copper smelting process. The material studied in this work is produced by Boliden AB as a commercial product called Järnsand ("iron sand") which is a water-granulated slag consisting of particles in the size range 0-2 mm.
- **Magnetite fines (MAF).** MAF is a concentrated ore product. It's a primary intermediate product sold for steelmaking and has a high iron content. The material studied here is produced by LKAB and consists of particles up to a few mm in size.
- **LD-slag.** Linz-Donawitz (LD) slag or basic oxygen furnace slag is a by-product from the steelmaking process, where iron is processed into low-carbon steel. The material studied here is a product by SSAB with a particle size range of 0-7 mm.
- **Iron mill scale.** Iron mill scale is a by-product of the hot rolling of steel sheets. The material is produced by SSAB and sold as the product Glödskal.

More information about the materials (their composition and references to previous studies) can be found in Table 4. In all those materials, it is the iron content that is the main active part and responsible for the oxygen-carrying properties.

2.2.1. Chemical-Looping Combustion (CLC)

The transition away from fossil fuels is a necessary measure to limit the climate changes observed as a function of increasing CO_2 concentrations in the atmosphere. However, fossil fuels are today still the main energy source globally [10], and biomass- and waste-derived fuels are not only typically more expensive but also technically more challenging to combust, as discussed previously. Carbon Capture and Storage (CCS) is identified as a key technology for limiting global warming to 1.5°C, according to the IPCC special report on global warming published in 2018 [22]. CCS involves capturing CO_2 from fossil fuels and storing it, so it's

prevented from reaching the atmosphere, e.g. in geological formations. One step further is to use CCS in combination with biomass fuels. Biomass is regarded as a CO_2-neutral energy source, since it captures CO_2 when it grows. Storing the CO_2 produced from biomass combustion can therefore be regarded as negative CO_2 emissions. This concept is referred to as Bio-Energy Carbon Capture and Storage (BECCS) [23].

The flue gas from conventional combustion contains mainly CO_2, N_2, and some oxygen, but pure CO_2 is required for CCUS. Post-combustion CO_2-capture is one alternative. For example, CO_2 absorption by amine-based liquid is a commercially available technology [23]. The drawback with amine absorption is that the process is energy-intensive and reduces the overall energy efficiency of the plant. What would make CCUS more attractive is finding an efficient technology for producing pure CO_2, without large energy penalties. CLC is one such technology, where oxygen carriers are used to produce a CO_2 stream that is not diluted with N_2 and O_2 inherently in the fuel conversion process. Using oxygen carriers for the production of pure CO_2 was first patented in the 1950s by Lewis and Gilliland [24]. They suggested using a copper oxide-based oxygen carrier and either a fluidized or moving bed reactor. Ishida et. al developed the process further and named it Chemical-Looping Combustion [25]. The concept is illustrated in Figure 3.

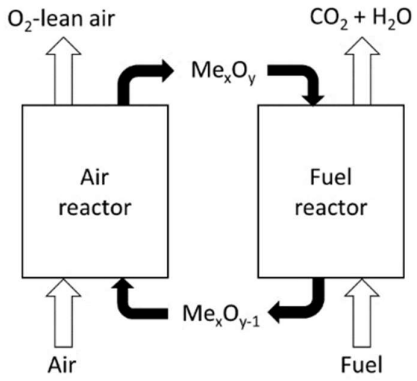

Figure 3: *Illustration of the CLC concept*

In the CLC process, the oxidation of the fuel and the oxidation of the oxygen carrier (for example according to Reaction (1) and (2) presented earlier) are separated into two reactors, referred to as the fuel reactor and the air reactor. The oxygen carrier is transported back and forth between the two reactors in a circular manner. As seen in Figure 3, the fuel conversion products (CO_2 and H_2O) are separate from the air. Pure CO_2 is obtained during cooling of the fuel reactor outlet, when steam condenses to liquid water.

The CLC process can be realised in two interconnected fluidized bed reactors. The air reactor resembles a CFB reactor, where high gas velocities cause entrainment of the particles to a cyclone. In the cyclone, the gas and the particles are separated. The particles then fall into the fuel reactor, which in its simplest iteration can have a lower gas velocity, more like a BFB reactor. From the fuel reactor, the particles exit from the bottom and fall back into the air reactor. Between the reactors are located loop seals, that stop the gas from one reactor to reach the other. Mixing of the gases or entrainment of fuel particles to the air reactor is undesirable, as it negatively affects the total carbon capture. The main heat extraction is in and downstream of the air reactor, as the oxidation of the oxygen carriers is strongly exothermic and

the gas flow is much larger, compared to the fuel reactor. The circulation of solids should be high enough to transport oxygen and heat throughout the system. Unit designs and process parameters will not be further discussed in this thesis but have been discussed extensively elsewhere (Adánez et al. [26], Lyngfelt & Leckner [27], Lyngfelt et al. [28] and Lyngfelt [29], to mention a few). To date, the largest demonstration of CLC has been in an autothermal 5 MW unit in China, with coal and pet coke as fuel [30], [31]. The largest scale of solid fuel biomass-CLC has been demonstrated in a 1 MW pilot plant in TU Darmstadt [32]. Truly industrial-size CLC is, however, yet to be realized.

Much of the early CLC development was focused on gaseous fuels [14]. Gaseous fuels can be injected into the bottom of the bed and make up the fluidizing gas. The fuel will be in immediate contact with the oxygen carrier and directly converted to the combustion products. In solid fuel-CLC, which is being developed more recently and may be of higher commercial relevance [15], [17], [26], [29], [33], the fluidizing gas in the fuel reactor is steam, or a mixture of steam and recirculated CO_2, to enable the gasification of the fuel char [15]. The solid fuel conversion with oxygen carrier in the absence of gaseous oxygen is illustrated in Figure 4.

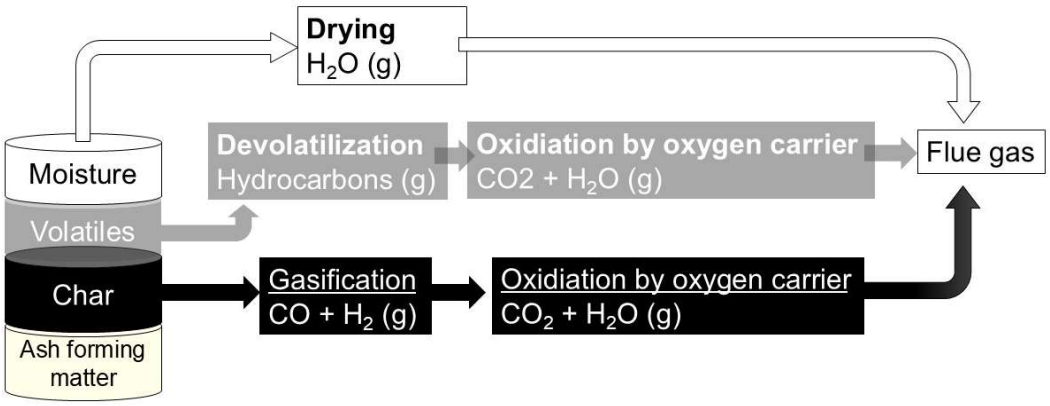

Figure 4: *Solid fuel conversion in CLC with oxygen carrier and no gaseous oxygen.*

In the absence of gaseous oxygen, there is no direct char combustion, as solid-solid reactions have a low probability of occurring [9]. Char gasification is by far the most time-consuming step in solid fuel CLC [34], [35]. Some oxygen carriers can release gaseous oxygen in reducing conditions, and can be applied in a process called Chemical-Looping Oxygen Uncoupling (CLOU) [26], [36]. In CLOU, the char is partly converted directly via char combustion. CLOU oxygen carriers include Cu and Mn-based materials. These will not be discussed further in his work.

2.2.2. Oxygen Carrier Aided Combustion (OCAC)

Conventional FBC suffers from some non-ideal mixing and fuel-oxygen contact, which can result in uneven temperature profiles and emissions of unconverted fuel components. As the fraction of volatile hydrocarbons is high in biomass and waste-derived fuels, the volatiles are released early in the conversion process, typically before the fuel has had time to become dispersed in the bed [37]. This creates a volatile rich zone close to the fuel-feeding location [37], [38]. By running the boiler at higher than stochiometric air-to-fuel ratios, large emissions of CO and hydrocarbons can anyway be avoided. However, the excess airflow is related to unavoidable thermal losses.

When using an oxygen carrier as bed material, the conditions in the boiler change as one more mechanism for fuel conversion is added. As the oxygen carrier can oxidize or reduce depending on the local oxygen partial pressure, the fuel can be converted even if there's locally a shortage of gaseous oxygen [39]. Thus, the introduction of oxygen carriers to FBC enhances the process by increasing the availability of oxygen in the boiler. The oxygen carrier also works as an oxygen buffer, meaning that a sudden temporary increase in fuel load could be managed by oxygen stored in the bed [37]. This is relevant for fuels that might have a wide range of heating value and moisture content.

OCAC was introduced in 2012 and was first demonstrated in Chalmers semi-industrial scale CFB research boiler by exchanging a part of the inert silica sand bed with ilmenite [6]. The operation was successful and the air-to-fuel ratio was reduced without increasing CO emissions [6]. Further, the air supply is often the limiting factor for the boiler load, so in practice, a reduced air-to-fuel ratio allows for increased thermal load in the boiler. In one 75 MW_{th} MSW-fired CFB boiler, the air surplus could be decreased by 25% and the load increased by 13%, when using ilmenite instead of silica sand as bed material [39]. By changing to ilmenite, another 115 MW_{th} wood-fired CFB boiler could lower the air surplus by 30% and increase the load by 7% [40]. The OCAC concept has been commercialized by the Swedish company Improbed AB, which is a subsidiary of the utility company E.ON. A summary of large-scale OCAC operation is presented in Table 1, showing several instances of operation with ilmenite and a few studies with LD-slag or manganese ore as oxygen-carrying bed materials. An important finding from the previous studies was that changing the bed material from silica sand to ilmenite in existing boilers often could be done more or less directly, and no major adaptation of the boiler was required.

Table 1: *Review of large-scale OCAC operation. For more context, see* ***Paper IV*** [5].

Oxygen Carrier	Facility	Description	Ref
Rock Ilmenite	Chalmers (12 MW_{th} CFB)	OCAC proof of concept study	[6], [41]
Rock Ilmenite	Chalmers (12 MW_{th} CFB)	Various OCAC research activities	[37], [42], [43], [44], [45], [46], [47]
Sand ilmenite	Chalmers (12 MW_{th} CFB)	OCAC research activities	[45]
Rock Ilmenite	Chalmers (4 MW_{th} gasifier)	CLC/CLG proof of concept	[48]
Rock Ilmenite	Händelö P14 (75 MW_{th} CFB)	OCAC in a commercial boiler	[39], [49]
Rock Ilmenite	Händelö P15 (85 MW_{th} CFB)	OCAC in a commercial boiler	[49]
Rock Ilmenite	Örtofta (115 MW_{th} CFB)	OCAC in a commercial boiler	[40], [47]
Rock Ilmenite	Eskilstuna (50 MW_{th} CFB)	OCAC in a commercial boiler	NA
Rock Ilmenite	ÖrebroP5 (170 MW_{th} CFB)	OCAC of a commercial boiler	NA
Rock Ilmenite	Sollefteå (19 MW_{th} BFB)	OCAC in a commercial boiler	NA
Rock Ilmenite	Borås (20 MW_{th} BFB)	OCAC in a commercial boiler	NA
LD-slag	Chalmers (12 MW_{th} CFB)	OCAC proof of concept study	[50], [51], [52]
LD-slag	Chalmers (4 MW_{th} gasifier)	CLC/CLG proof of concept	[53]
LD-slag*	Sävenäs HP2 (95 MW_{th} BFB)	OCAC in a commercial boiler	NA
Sibelco Mn-ore	Chalmers (12 MW_{th} CFB)	OCAC proof of concept study	[54], [55]
Sibelco Mn-ore	Chalmers (4 MW_{th} gasifier)	CLC/CLG proof of concept	[48]
Elwaleed C Mn-ore**	Chalmers (12 MW_{th} CFB)	OCAC research activities	NA
Foundry slag	Lidköping Energi (13 MW_{th} BFB)	OCAC in a commercial boiler	[56], [57]

* LD-slag inventory was only about 7% due to problems with the pneumatic transport of LD-slag.
**lasted only one day due to extensive elutriation of bed material.

To summarize the progress of the technologies: If suitable oxygen carriers are available at a reasonable cost, transitioning from conventional FBC to OCAC operation could likely be done without much effort. Such a shift could result in significant improvements in existing boiler stock, such as increased load and efficiency, and reduced emissions. Extensive retrofit of installed equipment likely wouldn't be required when changing from silica sand to an oxygen carrier. On the other hand, a scale-up of CLC to a truly industrial scale is yet to be demonstrated.

The development steps from conventional FBC to OCAC and CLC is illustrated in Table 2. OCAC could act as an intermediate step in the development of CLC. This is because the implementation of CLC would benefit from (i) an already existing market for oxygen carriers and (ii) deeper knowledge about oxygen carrier-ash interactions. While not necessarily equal in all aspects, the study of ash interactions taking place in OCAC conditions are relevant also for CLC. In the following sections, the use of oxygen carriers will be discussed mainly in the context of OCAC, because this is believed to be the most immediate application of oxygen-carrier technology. However, the discussion and the conclusions are likely to be relevant for the development of CLC as well.

There are almost uniquely favourable preconditions for utilizing oxygen carriers and developing CLC in Sweden. There are well-established metallurgical industries producing large amounts of products and by-products containing iron oxides [58]. Lyngfelt & Linderholm [17] further argue that the initial up-scaling of CLC should be based on upgrading existing CFB boilers. The development would therefore benefit from the already widespread utilization of FBC for solid fuel conversion and a large knowledge-base about fluidized bed processes [5].

Table 2: *Overview of the development from FBC to CLC.*

Fluidized Bed Combustion (BFB/CFB)	**Oxygen Carrier Aided Combustion (OCAC)**	**Chemical-Looping Combustion (CLC)**
	Fundamental design change ▪ Minor retrofit of existing FBC plants: Oxygen carrier constitutes the bed material	**Fundamental design change** ▪ Fundamentally new design: Conversion is separated into fuel reactor and air reactor
Conventional setup	**Main effects** ▪ Additional heterogenous (solid-gas) oxygen-fuel reaction ▪ Oxygen buffering in time and space ▪ Enhanced fuel conversion even at low air-to-fuel ratios ▪ Increased boiler load ▪ Lowered CO emissions ▪ Increased efficiency	**Boiler effects (main)** ▪ Inherent separation of CO_2 from other flue gases ▪ Zero or negative CO_2-emissions when connected to CO_2-storage

2.3. Biomass ash interactions with bed materials

As mentioned previously, there are some significant differences between coal and biomass and their properties as fuels in an FBC boiler. One of the main differences lies in the ash fraction of the fuels. Both the size of the ash fraction (as seen in the ultimate analysis in Figure 2) and the ash composition differ greatly, and this affects the conversion process. Some examples of ash composition are presented in Figure 5, showing representative compositions of ash from coal, wood, and straw grasses. The compositions are presented as oxides, although the actual composition will contain several different anions. The data is from *Åbo Akademi University Chemical Fractionation Database* [59]. The chart for coal shows mainly oxides of Si, Al, Fe, and Ca. The ash-forming elements in coal can accumulate in the fluidized bed without necessarily causing any operational problems. The challenges with coal combustion instead lie in the inherent production of fossil CO_2, formation of particulate matter, and SO_x emissions.

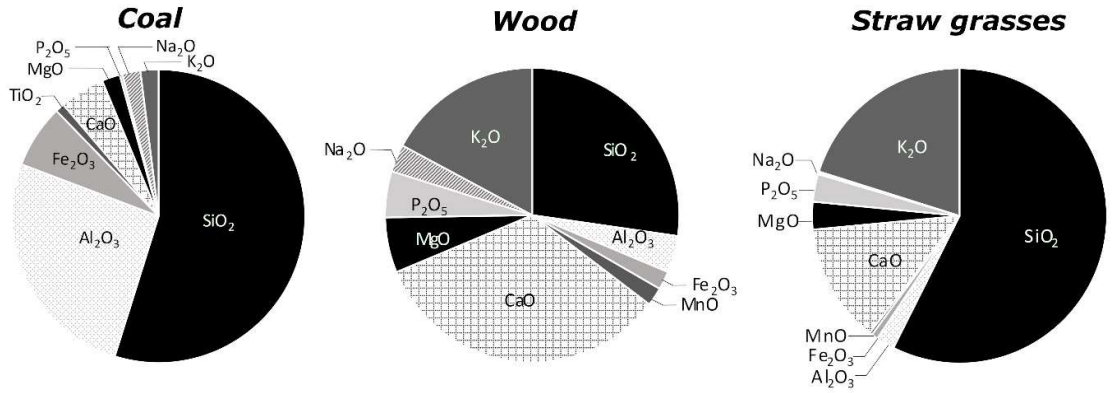

Figure 5: *Composition of coal ash, wood ash, straw grasses ash (wt.-%). The components are presented as oxides, and the data is from Åbo Akademi University Chemical Fractionation Database* [59]

In contrast, the charts for woody biomasses and straw grasses show large fractions of K, Si, and Ca, as well as some Na and P. Especially K, Na, and P participate in many reactions in the boiler that potentially can result in slagging, fouling and corrosion on boiler surfaces [8], [12]. The P content in woody biomass and the straw grasses presented here is quite low, but P-rich fuels such as sewage sludge and various agricultural residues will likely become important energy sources when the competition over woody biomass increases in the future [60], [61]. Of the different ash components, the most problematic in combustion is alkali [8], especially K because it might be present at quite high concentrations. In biomass, K is present as soluble salts and organically bound to the char matrix. When entering the boiler with the fuel, alkalis are mainly released in the gas phase. The release depends on what counter ions are available [8], [62]:

- If Cl is available, K is readily released as KCl(g). KCl is highly corrosive, especially if liquid KCl is deposited on boiler surfaces.
- The formation of KCl can be hindered by the presence of S and the formation of K_2SO_4.
- In the presence of steam, KOH can form, and under reducing conditions, the presence of K(g) is also possible.
- KOH(g) and K(g) can condense and form particles of K_2SO_4 or K_2CO_3.

These species may then be transformed both in the gas phase as well as in reactions with solids or liquids in secondary processes. By analysing bed material samples [62], [63], [60], and by monitoring gas phase alkali [64], [65], [66], the release and transformations of K in the boiler have been described in many previous studies. Volatile alkali can contribute to slagging, fouling, and corrosion on the surfaces inside the boiler [12], [8]. Volatile alkali also inhibits the complete burnout of the fuel [67], [68]. If alkali is absorbed by the bed material, it can be removed by bottom ash extraction and prevented from accumulating in the boiler. However, it can also cause agglomeration in the bed, so a high enough bed replacement must be applied to avoid defluidization. Some build-up of alkali on the particles can also have a positive effect on the conversion due to the catalytic effect of K on char gasification [69]. The situation can be even more severe for the combustion of MSW, but the discussion then becomes more complex because the composition of MSW and other waste-derived fuels varies a lot. Notably, the ash content in waste-derived fuels can be very high, and for example, MSW can contain significant amounts of for example Pb, Zn, and Cu [70].

A simplified bed material balance over FBC boilers is illustrated in Figure 6, showing the difference between coal- and biomass-FBC. The inflow of minerals to the boiler is divided into Fuel minerals (ash-forming matter) and Bed material (for example silica sand bed material). In coal combustion, the amount of ash-forming matter is significant, and bottom ash extraction is mainly required to keep the bed surface at a stable level. The concentration of fuel minerals in the bed can be allowed to be quite high. In biomass combustion, on the other hand, the amount of ash in the fuel can be relatively low. A high extraction of bottom ash is anyway required to prevent the ash species from accumulating in the boiler, for the reasons outlined above. To close the material balance over the unit, the required bed material make-up flow is high in the combustion of biomass-FBC. As a rule of thumb, the bed material consumption is about 3 kg/MWh and 6 kg/MWh in biomass and MSW combustion, respectively, but the numbers vary significantly between different boilers and operators. Bed material consumption in FBC will be discussed further in section 4.

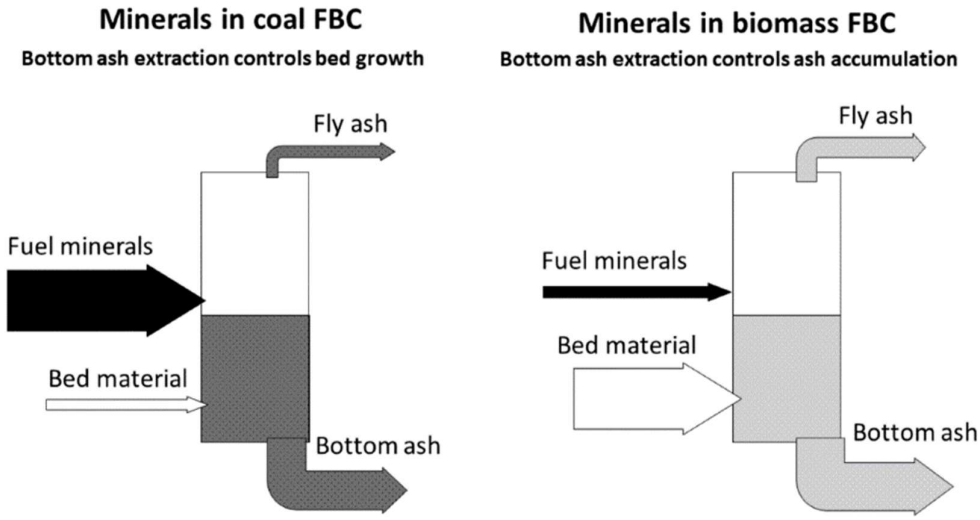

Figure 6: *Schematic representation of the mineral balance over coal and biomass-fired FBC boilers.*

Many studies have been performed to understand the mechanisms of agglomeration in fluidized-bed boilers and how it can be avoided [3], [71], [72], [73], [74], [75]. The initial agglomeration formation mechanism can be either coating-induced or melt-induced. An example of coating-induced agglomeration is when gaseous K-species attack silica sand particles, which results in a sticky melt formation on the surface of the particles [74]. $K_2Si_4O_9$ has been observed, which has a melting point of 770°C [76]. In contrast, a melt-induced agglomeration is initiated when a melt forms due to interaction between the ash species, for example from the burnout of a char particle containing both K and Si. This melt then adheres to the particle surface [69]. In both cases, the agglomeration happens because of sticky layers on bed particle surfaces, to which other bed particles get attached. K-silicate, and coating-induced agglomeration, is likely to form with quartz, but the interaction between K and Si depends on in what form Si exists in the bed material. Quartz, which has a network-like polymerized crystal structure of Si-oxide, is subject to depolymerization in the interaction with K resulting in melt formation [76], [77]. Other Si-rich materials, like feldspars and olivine, are rather subject to a substitution mechanism with Ca or Mg but are less likely to be subject to agglomeration due to K-silicates. However, they can still be subject to melt-induced agglomeration.

When melt has formed on the particle surface, other ash species such as Ca and Mg are incorporated into the melt, changing the composition of the layer. The incorporation of Ca can increase the melting point of phases that otherwise readily cause agglomeration. For example, if both K and P are present, they can form eutectic mixtures with melting temperatures as low as 590°C [60], [63], [78]. In the presence of Ca, however, K and P can be captured by Ca in phases with higher melting temperatures. The formation of $CaKPO_4$, $Ca_{10}K(PO_4)_7$ and $Ca_5(PO_4)_3OH$ has been reported in silica sand bed combustion with high-P fuels [73], [78]. Using limestone as an additive to the combustion can be a strategy for avoiding severe agglomeration. Note that the system is complex, and the mechanisms presented here are general. There are many other factors also influencing the final path of for example the K- and P-species in the boiler [73], [79].

Understanding the ash interactions with oxygen carriers in OCAC and CLC is crucial for developing the technologies. Ash interactions and particle ageing can have a large impact on the process and the economic viability of different oxygen carriers. Evidently, the interactions cannot easily be generalized, since they depend on the compositions of both bed material and ash. Ilmenite, being the most well-studied oxygen carrier in boiler settings, has been subject to material analysis to determine how the ash interactions change its morphology and composition [41], [42]. Agglomeration in ilmenite has not been observed, rather, K is known to diffuse into the ilmenite and become evenly distributed across the particles. The formation and stability of KTi_8O_{16} and $KTi_8O_{16.5}$ have been reported by means of XRD analysis of spent material [41] and thermodynamic calculations [80]. An ilmenite bed has been operated for over 300h without having to replace the material, but with magnetic separation of ash [47].

In the case of ilmenite, its interaction with K is considered positive for the process, due to the capture of volatile alkali in a form that doesn't induce agglomeration. The same mechanism has not been found with LD-slag as oxygen carrier. Rather, the K didn't interact with the material much, which presumably resulted in high levels of volatile alkali in the boiler [50], [51]. High levels of volatile alkali were also observed in the boiler with manganese ore as an oxygen carrier [54], [55].

Apart from studying particles from biomass combustion, several studies have been done on interactions between oxygen carriers and ash model compounds. Some recent studies regarding the interaction between model ash compounds and Fe-oxide based oxygen carriers are listed in Table 3 (including **Paper I**, **II** and **III**, which are part of this thesis). Most of the interaction experiments in these studies are performed in fixed beds, but some papers apply fluidized beds. Fixed bed interaction experiments are simple and important for testing extreme conditions. A drawback, however, is that they don't take into account the movements in the bed and don't give realistic conditions for the ash-bed material contact. The study by Zevenhoven et al. [81] was published before the start of this thesis, and was done with a fluidized bed with dry air as fluidizing gas. While representing better the movement of the bed, that study didn't take into account the influence of the alternatingly reducing and oxidizing conditions in CLC and OCAC processes. As part of this work, a new method was developed that allows for capturing the effects both of fluidization and of reducing atmosphere.

Table 3: *List of experimental studies of interactions between iron oxygen carriers and ash model compounds (including the papers presented in this thesis)*

Study	Oxygen carrier	Model compound	Salt addition	Experiments	Temp
Fixed bed experiments					
Hildor et al. [82]	Ilmenite	K_2CO_3 K_2SO_4 KCl KH_2PO_4	Mixture 4wt.-% K	Reducing, wet Reducing, dry	850°C
				TGA cycles, wet TGA cycles, dry	850°C
Staničić et al. [83]	Synthetic ilmenite Hematite	$CaCO_3$ K_2CO_3 SiO_2	Mixture 50 at.-% salt	Air, dry Reducing, wet	900°C
Yilmaz and Leion [84]	Pure Fe-oxide	Several Na- and K-based oxides and synthetic ash mixtures	Mixture 10 wt.-% model compound	Air, dry Reducing, wet	950°C
Störner et al. [85] (**Paper I**)	Iron mill scale Steel slag	K_2CO_3 K_2SO_4 KCl KH_2PO_4	Mixture 4 wt.-% K	Reducing, wet TGA cycles, wet	850°C
Purnomo et al. [86]	Ilmenite Copper slag Steel slag Iron mill scale	K_2CO_3 K_2SO_4 KH_2PO_4	Mixture 4 wt.-% K	Mildly reducing, wet	900°C
Hildor et al. [87]	Ilmenite Steel slag Mixtures	K_2CO_3 K_2SO_4 KH_2PO_4	Mixture 4 wt.-% K	Reducing, wet	900°C
Chen et al. [88]	Synthetic Fe-Si and Fe-Al-oxide	CH_3COOK KCl K_2CO_3 K_2SO_4	Feeding of K-doped cellulose		900°C
Fluidized bed experiments					
Andersson et al. [89]	Ilmenite	KCl, NaCl KOH, NaOH K_2SO_4 Na_2SO_4	Injection of alkali aerosol particles	Alternating oxidizing and reducing	900°C
Lu et al. [90]	Ilmenite	KOH K_2CO_3	Injection of alkali solution	Air/inert	700-900°C
Zevenhoven et al. [81]	Ilmenite	K_2CO_3 K_2SO_4 KCl KH_2PO_4	Continuous feeding solid salt	Dry air	850°C 950°C
			Fixed bed, mixture	Dry air	850°C
Störner et al. [91] (**Paper II**)	Ilmenite	K_2CO_3	Continuous feeding solid salt	Alternating oxidizing and reducing	850°C 950°C
Störner et al. (submitted) (**Paper III**)	Copper slag Magnetite fines	K_2CO_3 KH_2PO_4	Continuous feeding solid salt	Alternating oxidizing and reducing	850°C 950°C
Xu et al. [92]	Ilmenite ore residue	K-acetate	Injection of KAc-solution	Air	850°C
			Fixed bed and TGA	Air	

* mixture = the sample has been prepared by mixing the oxygen carrier and a solid salt

3. Methods and materials

The intended utilization of oxygen carriers is a large-scale combustion process. However, large-scale OCAC experiments without sufficient previous knowledge about the material have large risks associated with them, as for example severe agglomeration would require down-time and might harm the equipment. In small-scale experiments, on the other hand, severe agglomeration is not a problem, and the reactor can be easily cleaned. On top of that, it's possible to simulate conditions that are difficult to observe in a large-scale setting. These might be selected to represent extreme local conditions in the boiler such as high temperatures due to hot spots, very high ash concentrations, or very reducing conditions. It's also possible to study ash interactions in more detail, as interactions with specific ash species can be studied in isolation. Figure 7 together with Table 4 gives an overview of the methods used, and the oxygen carriers studied in this work. Composition, origin and some references to previous studies with the oxygen carriers are presented in Table 4.

The work covered by this thesis started on a small scale. LD-slag and the iron mill scale product Glödskal were studied in fixed bed experiments with model ash compounds, and the results are presented in **Paper I**. The oxygen carrier and ash model compounds were premixed and had close contact for a long duration. This should represent a "worst-case" situation for the oxygen carrier when it comes to agglomeration. However, the exposure in this setup doesn't represent the main contact between bed material and ash species in real boiler conditions, where not only is the bed fluidized, but the material is also subject to both oxidizing and reducing conditions and ash species concentrations increase continuously. To better simulate this, a new method was developed. Previous, fluidized fuel conversion experiments at this scale have been conducted in quartz glass reactors, but high concentrations of alkali would react with the glass, causing corrosion. A high-temperature steel fluidized bed reactor was therefore constructed, and ash model compounds were fed during experiments to simulate increasing ash concentrations over time. This method was used to study K-interactions with Ilmenite, Järnsand, and MAF. The studies are presented in **Paper II** and **III**. The ash model compounds used for the fixed and fluidized bed studies are presented in Table 4. Interactions with K_2CO_3 and KH_2PO_4 will be presented here, but some findings regarding KCl and K_2SO_4 exposure were also presented in **Paper I**.

Even though lab-scale experiments can provide useful insights into the chemistry of the material, they cannot truly demonstrate the real conditions in the boiler, where the particles are subject to more mechanical wear and exposed to the full range of ash species in the fuel. Based on the experimental findings in **Paper III** and the discussion in **Paper IV**, it was determined that copper smelter slag would be a suitable candidate to apply to a large-scale setting. Thus, as the final part of this work, a semi-commercial boiler was operated with the copper smelter slag product Järnsand as bed material. The general operability of the material and its oxygen-carrying effect in the boiler was evaluated. It was also studied how the material aged with exposure in the boiler. The findings from the semi-industrial scale experimental campaign are presented in **Paper V**.

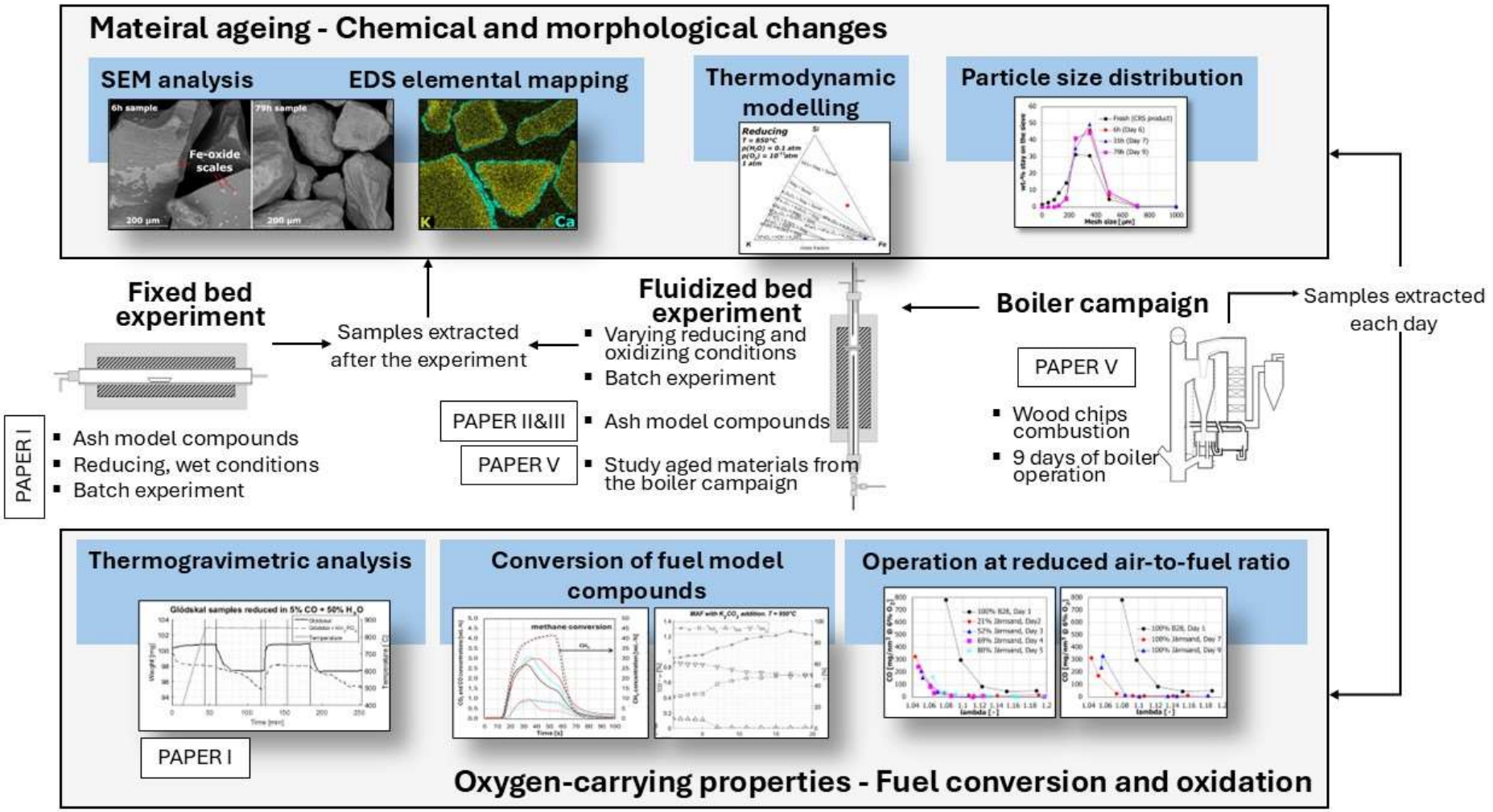

Figure 7: *Overview of the methods used in this thesis and examples of the data generated in the experiments.*

Table 4: *Oxygen carriers studied in the experimental work in this thesis.*

Oxygen carrier	Industrial process	Composition*							Origin	Experimental activity in this work	Previous research[e] and appended paper
Copper smelter slag (Järnsand)[a]	By-product from copper smelting	Fe	Si	Al	Ca	Zn	Mg		Boliden AB	Fluidized bed experiments, exposure to K_2CO_3 and KH_2PO_4	**Paper III** [86], [93], [94],
		34.6	18.6	2.87	2.39	1.04	1				
		Cu	Na	K	S	Mn	Cr			OCAC operation in 12MW_{th} boiler	**Paper V**
		0.58	0.55	0.48	0.4	0.3	0.16				
Ilmenite concentrate [b]	Mined for Ti-production	Fe	Ti	Mg	Si	Al	Ca	Mn	Titania A/S	Fluidized bed experiments, exposure to K_2CO_3 (**Paper II**)	**Paper II** [6], [95], [96]
		36.46	26.89	2.16	0.93	0.34	0.23	0.19			
LD-slag [c]	By-product from steel converter	Ca	Fe	Si	Mg	Mn	V	Al	Ti	SSAB	Fixed bed experiments and TGA. Exposure to KCl, K_2CO_3, K_2SO_4, and KH_2PO_4 (**Paper I**)	**Paper I** [50], [97], [98], [99],
		49.5	24.0	10.2	6.5	3.6	3.3	1.3	1.1		
Iron mill scale (Glödskal B) [c]	By-product from steel processing	Fe	Si	Mn					SSAB	Fixed bed experiments and TGA. Exposure to KCl, K_2CO_3, K_2SO_4, and KH_2PO_4	**Paper I** [21], [35], [100],
		95.1	4.0	0.9							
Magnetite fines (MAF) [d]	Ore concentrate	Fe_3O_4	SiO_2	Al_2O_3	MgO	CaO	TiO_2	V_2O_5	LKAB	Fluidized bed experiments, exposure to K_2CO_3	**Paper II**
		98.1	0.7	0.3	0.3	0.2	0.3	0.3			

[a] = Composition determined by total elemental analysis of bed material sample. Analysis was done externally by ALS Scandinavia. The analysis method is described in section *3.2*

[b] = Composition is according to product specifications (Titania A/S). Balance is mainly oxygen

[c] = Oxygen free composition. Composition determined with SEM/EDS analysis on a cross-section of many particles.

[d] = Composition is according to product specification (LKAB).

[e] = The list is non-exhaustive

* Trace amounts (< 0.1) are omitted, full compositions are provided in the papers

3.1. Lab scale exposure experiments

3.1.1. Fixed bed and reducing conditions

The reactor used for the fixed bed experiments was a cylindrical quartz glass vessel placed in a horizontal furnace. An illustration is presented in Figure 8. The reactor was equipped with a preheater that produced steam and heated the ingoing gas mixture to around 300°C. The results from the fixed bed exposure experiments are presented in **Paper I**.

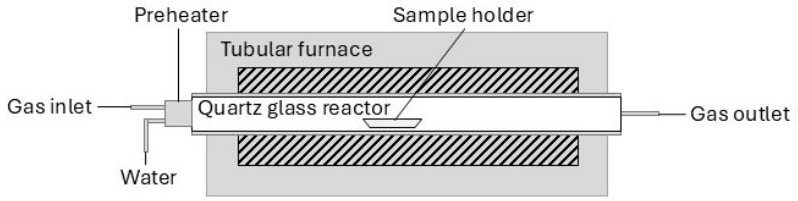

Figure 8: *Experimental setup for the fixed bed interaction experiments presented in* ***Paper I***

The procedure of the experiment was as follows:

- A mixture of an oxygen carrier (calcined at 950°C for 12h) and a K-salt was prepared so that the K-content in the mixture was 4 wt.-%. The particles were crushed finely in a mortar to facilitate solid-solid contact between the two components.
- 1 g of oxygen carrier-salt mixture was placed in a ceramic crucible and placed in the glass vessel. The gas lines were connected.
- The furnace was heated to 850°C with a heating rate of 15°C/min while 450 NmL/min N_2 was fed to the reactor.
- The inert flow was replaced by 500 NmL/min steam, 450 NmL/min N_2, and 50 NmL/min CO. The reducing, hot conditions were kept for 6 hours, then the reactor cooled down overnight with a flow of N_2. The samples were then subject to material analysis.

3.1.2. Thermogravimetric analysis (TGA)

Thermogravimetric analysis (TGA) was used for analysing the reduction and oxidation behaviour of oxygen carriers mixed with a model ash compound. In TGA, a small amount of sample is placed in a crucible which is continuously weighted. The setup is equipped with a furnace and gas connections, to allow for careful control of the environment in the reactor. In the current study, by altering between oxidizing and reducing conditions, it was studied what effect the different ash model compounds had on the oxidation and the reduction of the oxygen carriers. The following procedure was used for the experiments:

- A mixture of oxygen carrier and model ash compound was prepared in the same way as for the fixed bed experiments.
- 100 mg of the sample was placed in the TGA crucible.
- The system was heated to 850°C with a heating rate of 15°C/min while 1000 NmL/min N_2 was fed to the reactor. The inert flow was kept for another 15 min to allow the system to stabilize.
- The inert flow was replaced by 500 NmL/min steam, 450 NmL/min N_2, and 50 NmL/min CO. The reducing conditions were kept for 60 minutes.
- The system was flushed for 5 minutes with 1000 NmL/min N_2.

- The inert flow was replaced by 200 NmL/min O_2 and 800 NmL/min N_2. The oxidizing conditions were kept for 30 minutes.
- The reactor was again flushed for 30 minutes with N2, followed by another 60-minute-long reduction.

3.1.3. Fluidized bed with varying oxidizing and reducing conditions

The fluidized bed reactor was constructed from high-temperature 253MA-steel. A schematic view of the rector is presented in Figure 9. It consists of two pipes with an inner diameter of 26 mm connected in series. Between them is placed a perforated stainless-steel plate acting as a gas distribution plate. For the exposure experiments, the reactor was equipped with a solids-feeding port with an airlock. Sweep gas was connected to the feeding port so that inert gas could be used to flush the particles into the reactor. The reactor was placed in a furnace, in a larger experimental infrastructure described in detail by Leion et al. [101]. The reactor inlet was connected to a line for gas feeding. The outlet was connected to a gas analyser measuring the flow rate and the gas concentrations of CO, CH_4, CO_2, H_2, and O_2. The gas flow was controlled by mass flow controllers. Magnetic valves were used for seamless switching between different gas mixtures.

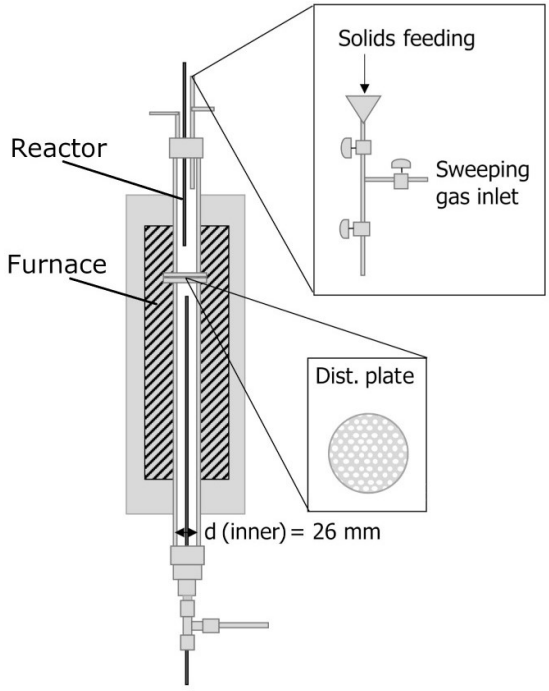

Figure 9: *Schematic drawing of the lab-scale fluidized bed reactor used in* ***Paper II, II*** *and* ***V***

The procedure of the experiment was as follows (slightly different conditions were used to study the boiler samples from the large-scale campaign, see **Paper V** for details):

- 20 g oxygen carrier (calcined at 950°C for 12 h and sieved to a particle size of 125-180 µm) was placed in the reactor. The reactor was placed in the furnace and the gas lines were connected.
- The sample was subject to cycles of syngas and air under increasing temperature up to the experiment temperature, until the reactivity stabilized (activation).

- The reactor was heated to 850 or 950°C (experiments were conducted at both temperatures).
- The first reduction was started, and the program in Table 5 was followed.
- Before the 6th reduction, the model ash compound was added (K_2CO_3 or KH_2PO_4). Salt was then added every second cycle. For example, the addition amounts given in Table 6 were used for the experiment with ilmenite and K_2CO_3. A lower rate was used in the experiments with Järnsand, see **Paper III** for details.

Table 5: *Program used in the experiment with salt addition during CLC cycles.*

Period	Gas flow (NmL/min)	Gas composition	Time
Start of experiment cycles			
Reduction	400 NmL/min 500 NmL/min	CH_4 N_2	40 s
Inert	1000 NmL /min	N_2	60 s (approx.)
Oxidation	1000 NmL/min	Air in N_2 (12.4% O_2)	Until outlet = inlet O_2 concentration
Inert*	1000 NmL /min	N_2	180 s (approx.)
* K_2CO_3 was added to the bed during this inert period preceding the reduction.			

Table 6*: Details of the additions of K_2CO_3 during the experiment with ilmenite.*

Cycle no.	Addition (mg)	Accumulated (mg)	Wt.-% salt added to the bed	Wt.-% K added to the bed
6	100	100	0.5	0.3
8	100	200	1.0	0.6
10	300	500	2.4	1.4
12	400	900	4.3	2.4
14	400	1300	6.1	3.5
16	500	1800	8.3	4.7
18	500	2300	10.3	5.8

To quantify and compare the fuel conversion in the fluidized bed experiments, the following parameters were calculated from the concentrations measured in the reactor outlet:

- **Mass-based conversion.** The mass-based conversion of the oxygen carrier is defined according to Equation (1), where m is the mass of the oxygen carrier and m_{ox} is the mass of the fully oxidized oxygen carrier.

  $$\omega = \left(\frac{m}{m_{ox}}\right) \times 100\ [\%] \qquad \text{Equation (1)}$$

  The mass-based conversion at a given time is calculated according to Equation (2), where ω_i is the mass-based conversion at the beginning of the reduction (ω_i is assumed to be = 1, i.e. the oxygen carrier is fully oxidized), M_o is the molar mass of oxygen, x is the gas concentration, and $\dot{n}$ is the molar flow (moles/second).

  $$\omega = \omega_i - \left(\int_{t_0}^{t_1} \frac{\dot{n} M_o}{m_{ox}} \left(4x_{CO_2} + 3x_{CO} - x_{H_2}\right) dt\right) \times 100\ [\%] \qquad \text{Equation (2)}$$

The final mass-based conversion, ω_f, was defined and calculated with t_1= the length of the reduction. The mass-based conversion is presented as $100 - \omega_f$ in the results.

- **Gas yield.** The yield of CO_2 in the cycle was calculated according to Equation (3), where n_{CO_2} is the number of moles of CO_2 formed in the cycle.

$$\gamma_{CO_2} = \frac{n_{CO_2}}{n_{CO_2}+n_{CO}+n_{CH_4}} \quad \text{Equation (3)}$$

n_{CO_2} is calculated by integrating the molar flow of CO_2 over the whole reducing period according to Equation (4). n_{CO} and n_{CH_4} are calculated in similar ways.

$$n_{CO_2} = \int_{t_0}^{t_1} \dot{n} x_{CO_2} dt \quad \text{Equation (4)}$$

Similarly,

$$\gamma_{CO} = \frac{n_{CO}}{n_{CO_2}+n_{CO}+n_{CH_4}} \quad \text{Equation (5)}$$

$$\gamma_{CH_4} = \frac{n_{CH_4}}{n_{CO_2}+n_{CO}+n_{CH_4}} \quad \text{Equation (6)}$$

3.1.4. Ash model compounds

The ash interactions taking place in biomass- and waste-derived fuel combustion are very complex. To simplify the system and make the parameters easier to control, ash model compounds can be used instead. Some experimental studies using ash model compounds in the form of pure salts or mixtures of a few salts were presented in section 2.3.

In the current studies, K_2CO_3 and KH_2PO_4 were used as ash model compounds. The idea behind using those species was to (1) simulate the interactions with K in the absence of any other ash species, i.e. isolating the K-interactions by adding K_2CO_3, and to (2) observe the specific interaction with a K-P-specie, as this is related to very high risks of agglomeration.

K_2CO_3 is not likely a significant form of K inside the bed at combustion conditions, but using it as an ash model compound is useful for a couple of reasons. Based on previous studies and the findings in **Paper I**, K_2CO_3 is expected to partly decompose according to $K_2CO_3 \rightleftharpoons K_2O + CO_2$. The decomposition of K_2CO_3 is not straightforward, because it depends on the partial pressure of CO_2, the temperature and the competing formation of KOH in presence of steam [102], [103], [104], [105]. No external steam was added in the fluidized bed experiment, but steam was produced in the conversion of CH_4, thus some KOH formation should be possible. The release of K from K_2CO_3 under different conditions was investigated by Knudsen et al. [103]. They found that K was present as K_2CO_3 in the temperature interval 500-950°C or interacted with Si present. The carbonate fraction decreased at temperatures above 700-800°C because of the decomposition of K_2CO_3 in the presence of small amounts of H_2O and CO_2, but K_2CO_3 was more stable as high partial pressures of CO_2 [102]. In the TGA experiments presented in **Paper I**, K_2CO_3 started decomposing at 670°C in inert atmosphere. K_2CO_3 has a melting point of 891°C. The partial decomposition to K_2O and the presence of KOH in the reactor should be suitable reaction paths for K, as K_2O is unlikely to be stable and KOH likely evaporates. In conclusion, K_2CO_3 should be available for interactions with the bed material in the experiment, and at the same time, stable enough to reach the fluidized bed and have a significant residence time there. After initial testing with K_2CO_3 addition to ilmenite in the fluidized bed (presented in **Paper II**), it was decided based on initial material analysis that the addition method worked because K was found both in the interior and on the surface of ilmenite particles. At 850°C, the sample

contained much of the added salt as solid salt particles in the bed, this is seen also in Järnsand samples in Figure 10 and in MAF samples in Figure 18.

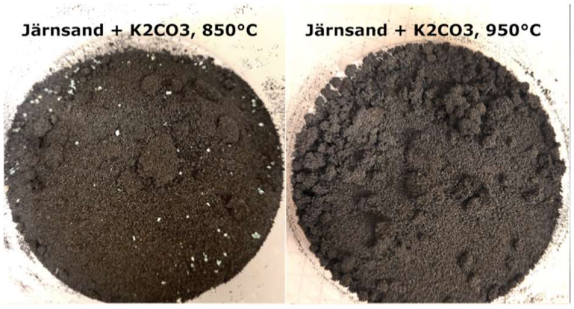

Figure 10: *Photos of samples of Järnsand from fluidized bed interaction experiments with the addition of K_2CO_3. The left photo (experiment was conducted at 850°C) shows white grains that were identified as K_2CO_3 in SEM-EDS analysis.*

If P is present, alkali-phosphates can form [60], [63], which is modelled in this study by KH_2PO_4. KH_2PO_4 has a melting temperature of 253°C and decomposes upon heating into KPO_3 and H_2O. KPO_3 has a melting temperature of 807°C and sticks to particle surfaces, resulting in melt-induced agglomeration. Some interaction experiments with ilmenite and iron oxide has been conducted, still, the Fe-K-P system is not yet well studied. [81], [82], [84].

In addition to K_2CO_3 and KH_2PO_4, the fixed bed interaction experiments were also conducted with KCl and K_2SO_4 but were excluded from the fluidized bed experiments. Another alternative could have been KOH.

- **KOH and KCl** are likely very volatile in the experimental conditions, thus a too short interaction time was expected with those. KCl is also very corrosive at high temperatures, and therefore using it was associated with a risk of harming equipment. Further, very little interaction was observed with KCl in the fixed bed experiment, likely because of a high evaporation rate.
- **K_2SO_4** decomposed slowly according to fixed bed and TGA, and very little interactions were observed.

3.2. Semi-industrial scale CFB-type research boiler

The facility used for the large-scale experiment is a wood-fired semi-commercial CFB boiler located at the campus of Chalmers University of Technology. The installed capacity of the boiler is 12 MW_{th} for coal combustion. Nowadays, the boiler is operated with wood chips of mainly stem wood from pine and spruce, at a load of around 5-8 MW_{th}.

A schematic representation of the boiler is presented in Figure 11. The furnace has a cross-section area of 2.25 m^2 and is 13.6 m high. Bed material sample extraction was done at H2.5, located between H2 and H3. The bottom bed temperature was fixed and controlled by flue gas recirculation. Thus, an increase in fuel feeding (and heat production) was related to an increase in flue gas recirculation to cool the bed. During the experimental campaign, no fuel was fed to the gasifier and most of the time, the gasifier was disconnected from the boiler. For practical reasons not related to the campaign, a circulation of bed material through the gasifier was required during the last three days of operation, and the bed material inventory was increased

from around 2000 to 3700 kg. Most of the time, the boiler was operated at nominal conditions to evaluate the general operability of Järnsand. To explore the oxygen-carrying ability of Järnsand, the boiler was temporarily operated at reduced air-to-fuel ratios. In practice, this was achieved by fixing the airflow and then increasing the fuel feeding rate by around 20-60 kg/h at a time. More details about the method, the boiler and measuring techniques are presented in **Paper V**.

The bed material used in the campaign was derived from the commercial product Järnsand 0/2 from Boliden. The material was crushed and sieved by Comminution Reimagined Sweden AB (CRS) and 16 tons of bed material was delivered to Chalmers. There were about 5 wt.-% fines smaller than 0.09 mm in the delivered material. According to CRS, this fine fraction could be removed by wind sieving, with only small amounts of extra effort, but no such equipment was available at the time. For the processing, a milling rather than a crushing technique was applied, and this resulted in high material yields (around 80%). The bulk density of the fresh material was 1.66 g/cm^3. The size distribution of Järnsand 0/2, and the final size distribution of the product are presented in Figure 12.

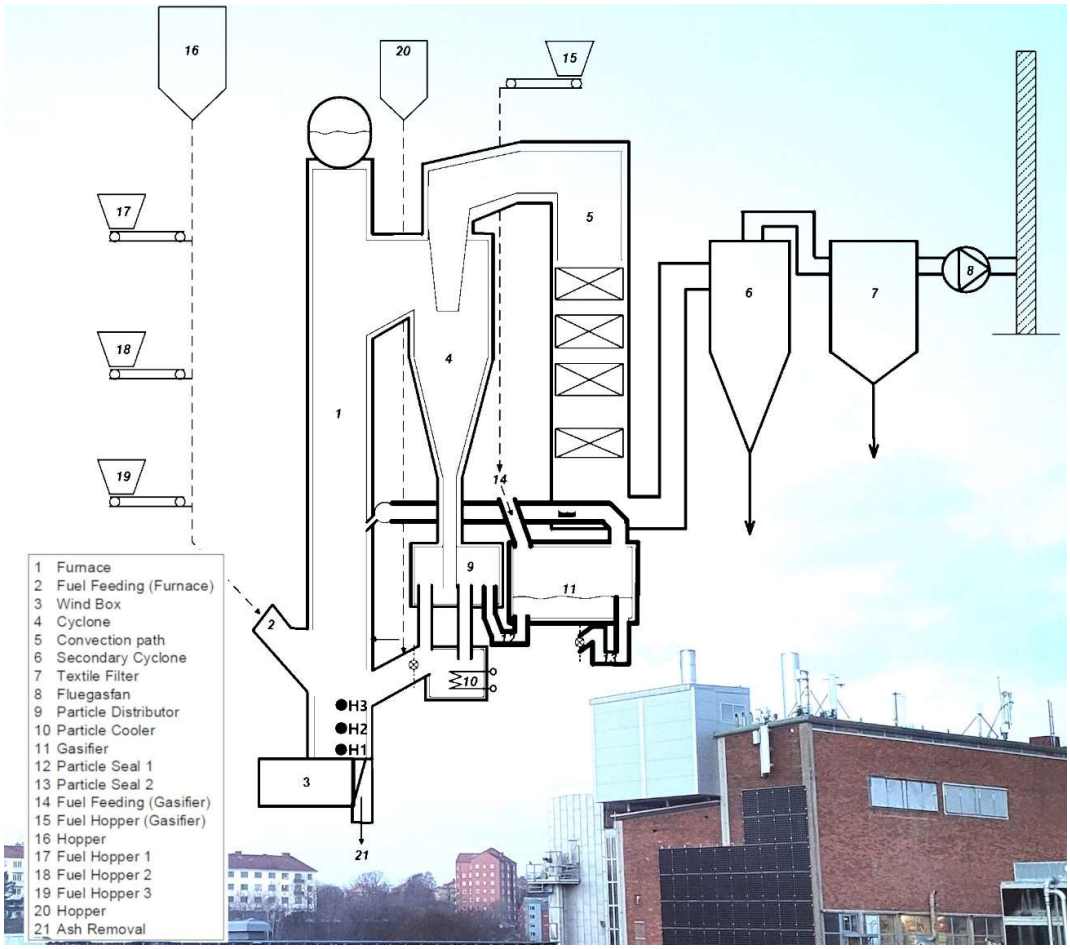

Figure 11: *A schematic representation of the Chalmers 12 MW$_{th}$ research boiler/gasifier. A photo of the boiler in the background.*

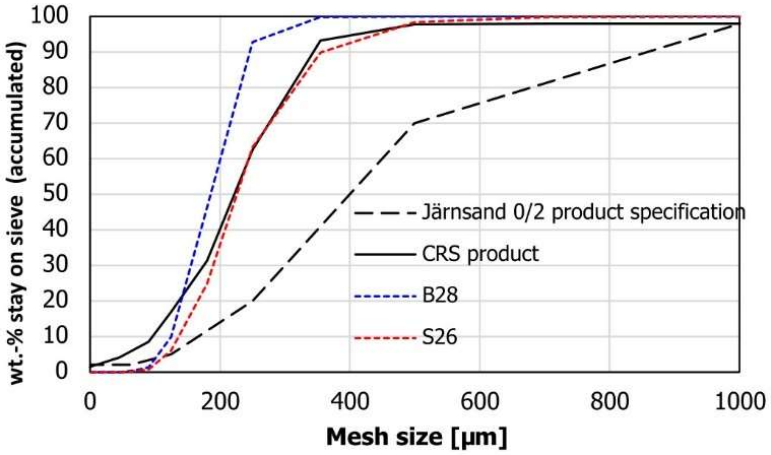

Figure 12: *Size distributions of the copper smelter slag product Järnsand 0/2 and the resulting size distribution after processing it into a bed material. B28 and S36 (common silica sand bed materials for CFB boilers) are included for reference.*

3.3. Material analysis

Samples exposed to the ash model compounds, or which had been aged in the boiler, were studied with different material analysis methods. A summary is presented here, and for more details on the methods, please see the respective appended papers.

- **SEM-EDS.** Scanning electron microscopy[1] (SEM) coupled with energy-dispersive X-ray analysis[2] (EDS) was used for analyzing the structure and the elemental distribution of particles. For surface analysis, the particles were mounted on a stub with carbon tape. For analyzing the cross-section, particles were placed in a mould together with epoxy and the epoxy slab was polished to obtain a cross-section. The method was used to study elemental distributions in individual particles but was also used to determine a bulk elemental analysis, measuring the elemental composition across several hundred particles at a time. For studying the ash layer on particles from the boiler exposure in more detail, a few particles were glued between two silica wafers and a very smooth surface was obtained using a broad ion beam (BIB) technique[3].
- **BET surface area.** The Brunauer-Emmett-Teller (BET) surface area[4] was measured by the method of gas adsorption.
- **XRD analysis.** X-ray Diffraction[5] analysis was conducted to determine the crystal structure of the materials.
- **Bulk elemental analysis.** The total elemental composition was analyzed by ALS Scandinavia AB with a standard method of dissolution in $LiBO_2$-melt (ASTM D3682:2013) or HNO/HCl/HF solution (SS-EN 13656:2003) and subsequent ICP-MS analysis (ISO 17294-2:2023)

[1] LEO Gemini 1530 or FEI ESEM Quanta 200
[2] Thermo Scientific UltraDry Silicon Drift Detector (SDD)
[3] BIB, Leica EM TIC 3X
[4] Micromeritics TriStar 3000 or Bruker D8 Discover
[5] Malvern Panalytical Empyrean diffractometer

3.4. Thermodynamic modelling

To better understand the experimental results in **Paper III**, complementary thermodynamic modelling was done using FactSage 8.2 [106]. As MAF is mainly Fe-oxide with small amounts of Si, and Järnsand is mainly Fe-Si-oxide, ternary Fe-Si-K phase diagrams were constructed. The databases FactPS and FToxid were used and $KFe_{11}O_{17}$ and $KFe_{10}O_{16}$ were included from a user-defined database [107]. The solution phases Slag-A, SpinA (spinel), MeO_A and cPyrA (pyroxene) were considered in the calculations. Four phase diagrams were created:

- The temperature was either 950 or 850°C
- The atmosphere was either reducing: $p(O_2) = 10^{-11}$, $p(H_2O) = 0.1$ atm or oxidizing: $p(O_2) = 0.13$ atm, $p(H_2O) = 0.01$ atm.

Predominant phases at oxidizing and reducing conditions of one of the samples were also modelled using the full elemental composition of the sample. This was done to determine if the other elements (such as Ca, Mg, and Al) influenced the interactions with K.

4. Results Part I: Interactions with ash compounds

The results in this section are focused on the K-interactions with the oxygen carriers and the findings from the lab-scale experiments. The results are divided into (i) interactions with Fe-oxide (MAF and Glödskal), (ii) interactions with Fe-Ti oxide (ilmenite) and (iii) interactions with slag (LD-slag and copper smelter slag). In the latter category, there are some similarities regarding the compositions but the alkali interactions and performance as bed materials differ. The interactions with KH_2PO_4 are discussed separately in the final part of this section. The presence of P significantly changes the behaviour of K, as the formation of low melting, sticky KPO_3 readily causes agglomeration. The interaction anyway depended on the composition of the oxygen carrier, sometimes causing a more severe agglomeration than in other cases.

From the K_2CO_3 exposure experiments, it was evident that the K interaction differed with different materials. In most of the experiments, some degree of agglomeration of the particles was observed. The Fe- and Fe-Ti-oxide materials were subject to solid-state sintering between Fe-oxide layers on the surface, a process which was enhanced by the addition of K_2CO_3. The agglomeration in LD-slag and Järnsand looked different, as the materials contain significant amounts of for example Si, Mg, Al, and Ca. Note that comparing the agglomeration quantitatively is difficult as the fixed and fluidized beds create very different conditions for the interactions.

4.1. Interaction between K and Fe-oxide

The results in this section are based on the fixed bed exposure and TGA experiment with Glödskal and different K-salts, and the fluidized bed experiment with MAF exposed to K_2CO_3. These oxygen carriers represent "pure" Fe-oxide, although the materials contain some Si and other minor elements, as seen in Table 4. The addition of K_2CO_3 affected both the reactivity and the morphology of the materials. Figure 13 shows how the fuel conversion of MAF in the fluidized bed experiment increased significantly with K_2CO_3 addition. In Figure 14, presenting the TGA results for Glödskal, it's evident that Glödskal mixed with K_2CO_3 had a more rapid reduction than the sample without K_2CO_3.

A change in the particle structure was especially pronounced for the MAF sample from the 950°C fluidized bed experiment – when removed from the reactor, the density had decreased by almost 40%, meaning that the particles had been subject to swelling. The same was not seen in the reference experiment without the addition of K_2CO_3. Figure 15 shows a few MAF particles from a K_2CO_3 addition experiment, and shows that the higher fragmentation was related to a higher K concentration. Figure 16 further shows the particle surface of Glödskal reduced in the presence of K_2CO_3, compared to without. The first seems more fragmented and the cracks on the surface are more pronounced.

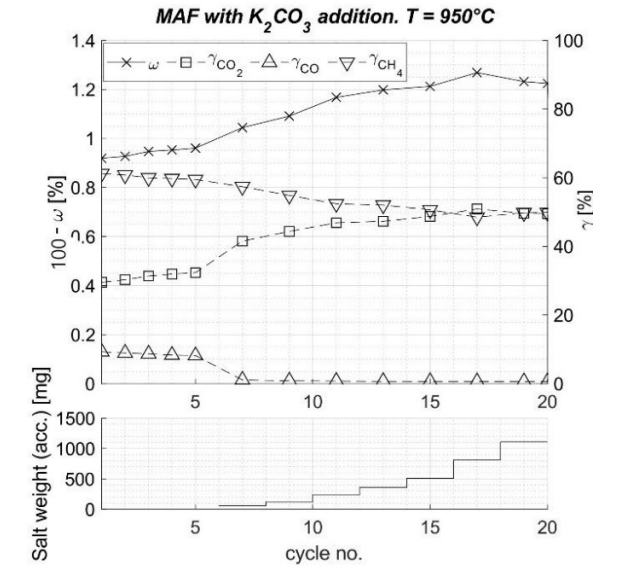

Figure 13: *Fuel conversion during the 950°C fluidized bed experiment with MAF as oxygen carrier and addition of K_2CO_3. The K_2CO_3-addition period is between cycle 6 and 18, which is related to increasing fuel conversion. ω_f is the mass-based conversion reached at the end of each reduction (100- ω_f is presented here). The parameters are explained in section 3.1.3.*

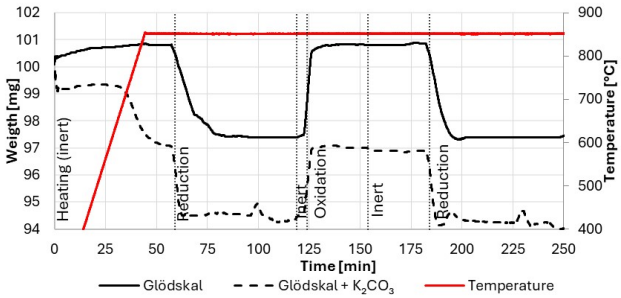

Figure 14: *Recorded weight change during the TGA with Glödskal and Glödskal mixed with K_2CO_3. The mixture with K_2CO_3 shows a more rapid reduction, suggesting a more reactive material. The initial weight change is related to the decompositions of K_2CO_3.*

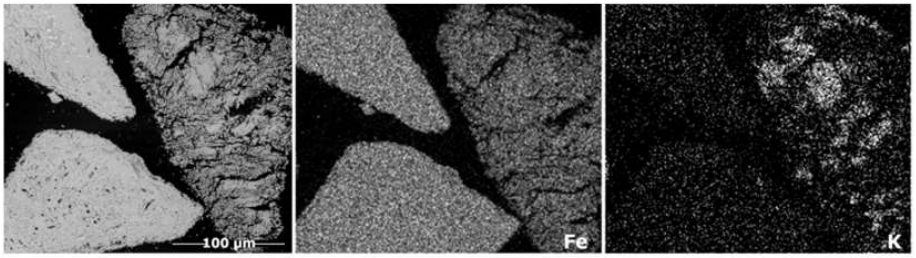

Figure 15: *MAF particles with K_2CO_3 added during the fluidized bed experiments. The analysis is SEM-EDS on cross-section of particles. The most porous particle to the right contains more K.*

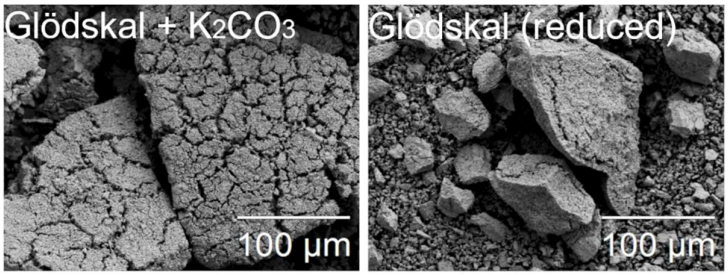

Figure 16: *Particles of Glödskal from fixed bed interactions. The particles reduced in the presence of K_2CO_3 (left) look more fragmented, with more pronounced cracks visible on the surface.*

It's likely that the increase in reactivity and the swelling/fragmentation of the particles were related, as a more porous structure would entail a higher contact between the solid phase and the gaseous fuel phase. In previously published research, increasing reactivity and simultaneously increasing surface area were observed for Glödskal during 25 cycles of reduction and oxidation[35], [100]. The experiments were conducted in a lab-scale fluidized bed reactor with syngas or methane as fuel, and the reactivity continuously increased without reaching steady operation. A development from robust, bulky Glödskal particles to thin, flaky fragments was also described by Moldenhauer et al. [21]. That experiment was conducted for 37 hours in a continuous lab-scale 300 W CLC reactor with syngas as fuel. The direct connection between surface area and increased reactivity is, however, not clear. An increased conversion of solid fuel was found by Gu et al. [18] when adding K_2CO_3 to an iron ore oxygen carrier. However, they found that the increased fuel conversion was attributed to changing the equilibrium of the water gas shift reaction towards producing more H_2 ($CO + H_2O \rightleftharpoons CO_2 + H_2$) and enhanced char gasification but did not observe increased conversion of CO alone. In a later study by Gu et al., [108] an increased conversion of CO was observed and also increased BET surface area with addition of K-rich ash, but the connection between reactivity and BET surface area was not obvious. They suggested that another contribution by the K was that the formation of K-Fe-O-phases changed the binding energy between the Fe and the O, making the oxide more prone to react with the fuel. Initially, fragmentation might be beneficial for fuel conversion. Unless the material maintains sufficient particle integrity, however, it will result in decomposition and loss of material. Indeed, the 300 W CLC study [21] concluded that the fragmentation led to a considerate material loss after 37 hours of operation. According to the current studies, the addition of K_2CO_3 accelerates this development. Note that the change in porosity or surface area has not been determined quantitatively in the current studies, for example by BET surface area measurements.

Interestingly, even though the reactivity and the morphology changed, the actual inclusion of K into the material was low, according to the SEM-EDS analysis of both Glödskal and MAF samples. On the other hand, the bulk elemental analysis showed that the K_2CO_3-exposed MAF samples contained 2 wt.-% K (after exposure at 950°C) and 3.4 wt.-% K (after exposure at 850°C). As discussed before, the addition of K_2CO_3 at 850°C resulted in salt particles remaining in the bed, seemingly without reacting, which explains the high concentration in the sample exposed at 850°C. However, the SEM-EDS analysis failed to identify the location of the K in the 950°C sample, as the analysis showed very low concentrations. Further, no K-containing phase could be determined from the XRD analysis for either material. According to the thermodynamic modelling and the ternary Fe-Si-K diagrams produced by presented in Figure 17, K interaction results in mainly the formation of slag. The predicted slag contains K_2O, SiO_2, and minor amounts of Fe_2O_3, $KFeO_2$, and FeO. At oxidizing conditions and/or higher K concentrations, the formation of $KFe_{11}O_{17}$ is possible. The composition of the MAF samples with K_2CO_3 exposure is represented by the blue triangle. Even though the concentration of K is low according to the SEM analysis, it's likely that the formation of K-Fe phases could cause changes in the crystalline structure which ultimately weakens the particle. This is supported by the higher K-concentration in the porous particle than in the denser particles (Figure 15). In a study by Yilmaz and Leion

[84], Glödskal and pure Fe_2O_3 and Fe_3O_4 were exposed to different K-salts in fixed bed experiments similar to this work, and they also concluded a low K-absorption by the pure Fe-oxides. In one case, with the addition of KNO_3 as a model compound to Fe_2O_3, they identified K_2FeO_4 in XRD analysis, but not other phases containing K.

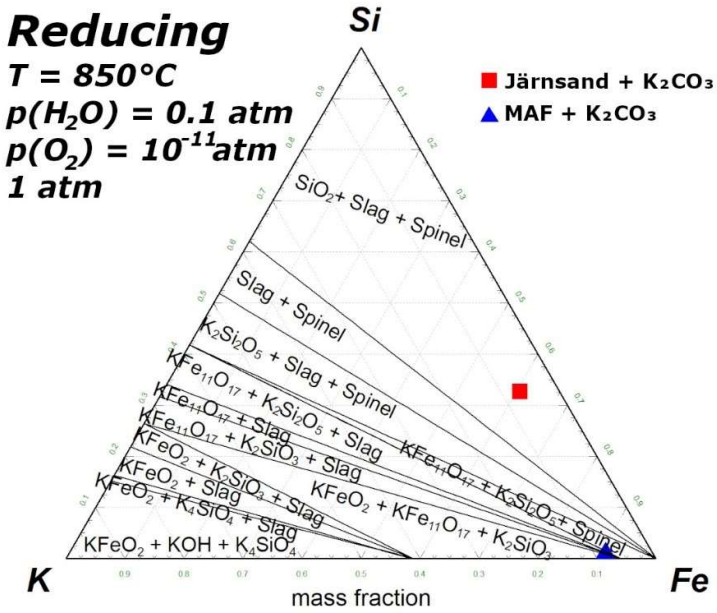

Figure 17: *Ternary Fe-Si-K phase diagrams at 850°C and reducing conditions. The red square and the blue triangle represent the composition of Järnsand and MAF respectively, after interaction with K_2CO_3 in the fluidized bed experiments.*

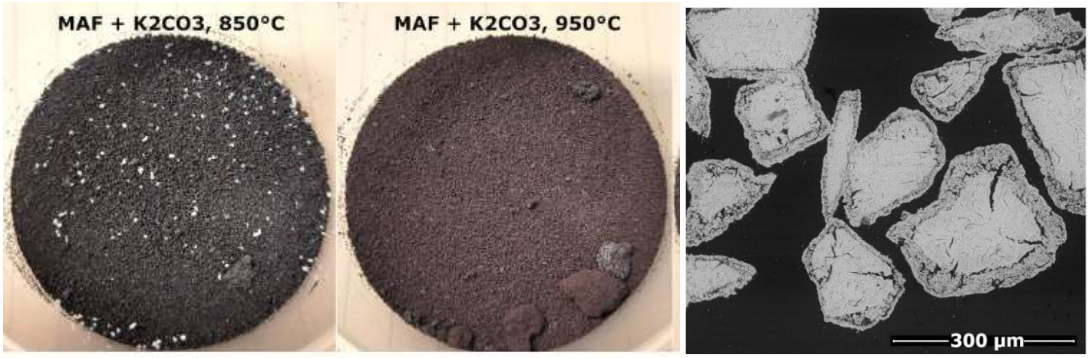

Figure 18: *Photos and a SEM micrograph of MAF after the experiments with addition of K_2CO_3. The SEM micrograph to the right shows some agglomerated particles from the 850°C experiment. Very low concentrations of K were detected with SEM-EDS.*

It was further found that the agglomeration tendency of MAF and Glödskal with K_2CO_3 addition was low, but higher than without K_2CO_3. In the fluidized bed experiments, the agglomeration tendency can be evaluated during the experiment, as the formation of agglomerates results in a defluidization of the bed, which is visible in the pressure drop measurements. The photos in Figure 18 show the samples from the fluidized bed experiments with MAF and K_2CO_3, showing some agglomeration but not to a large extent. During 850°C, a short period of defluidization was noticed, but not at 950°C. In neither Glödskal nor MAF were there any signs of a melt or a high K-

containing phase being responsible for the agglomeration, but rather that the porous Fe-layer on the particle surfaces had merged. An example is seen to the right in Figure 18.

4.2. Interaction between K and Fe-Ti-oxide (ilmenite)

The fluidized bed experiment with ilmenite demonstrated an uptake of K into the particles. This is seen in Figure 19. Apart from pseudobrookite, hematite, and magnetite, KTi_8O_{16} was detected in the XRD analysis and potentially, low amounts of other K-titanates could also be suggested. The pseudobrookite separated into Fe-oxide and K-titanate to a larger extent in the 950 than in the 850°C experiments. Absorption of K and formation of KTi_8O_{16} has been reported in the literature, when analysing ilmenite samples from boiler operation with woody biomass [41], [42], from fixed bed interactions with K_2CO_3 [82] or K-acetate [92], and from fluidized bed interactions with the injection of K_2CO_3-, KOH- [90], or K-acetate[92] solutions. In thermodynamic calculations by Corcoran et al. [42], and a higher K/Ti-ratio was predicted to be possible with the formation of $K_2Ti_3O_7$ and $K_2Ti_6O_{13}$, but these have not been identified in boiler samples. Faust et al. [107] observed the formation of $K_2Ti_6O_{13}$ from dedicated fixed bed K_2CO_3-interaction experiments with long exposure times and high K-concentrations.

In the fresh material, Fe was evenly distributed together with Ti but migrated to the surface of the particles during oxidation and reduction cycles. This mechanism was observed also in the absence of K and has been explained in previous works. The Fe migration to oxygen-rich surfaces and oxidation to Fe_2O_3 increases the fuel reactivity of ilmenite early in the process, which is referred to as activation [42], [109], [110].

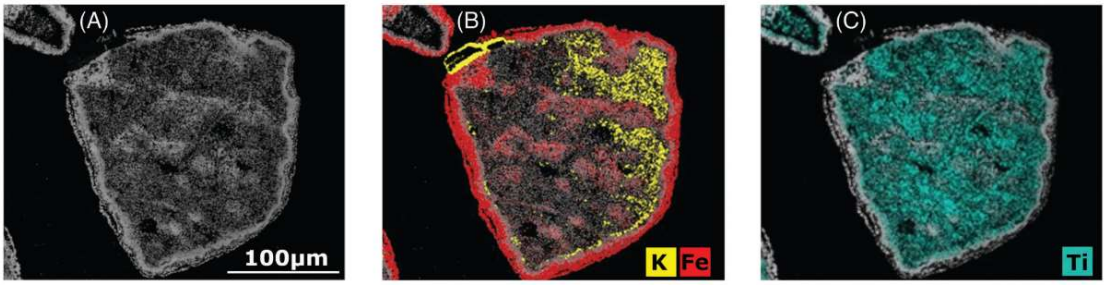

Figure 19: *An ilmenite particle after interaction with K_2CO_3 in the fluidized bed. The analysis is SEM-EDS on the cross-section. A layer of Fe on the surface and the enrichment of K underneath the Fe-layer is visible. Ti is distributed across the whole particle except for in the Fe-layer.*

Agglomeration was observed in the current study, when K_2CO_3 was added, and the reactor temperature was 950°C. This caused a defluidization of the bed after 12 cycles, as seen in Figure 23, after the addition of in total 900 mg of K to the reactor. The agglomeration mechanism was that Fe-layers formed on the particle surface and eventually sintered. This is visible in Figure 20. This agglomeration closely resembles what was seen with MAF exposed to K_2CO_3. Similar agglomerations has been reported before in ilmenite, with either the addition of K_2CO_3 [81] or at highly reducing conditions [20]. There is no evidence that any eutectic point exists in the Fe-Ti-K system at the studied K-concentrations, and no melt has been observed in this or reported studies. The agglomeration is rather through solid-state sintering on the surface. The contribution of K_2CO_3 in this agglomeration mechanism is as suggested in Figure 21: the inwards diffusion of K enhances the migration of Fe to the surface, which in turn increases the risk for solid-state sintering between particles. The mechanism has similarities with the

industrial process known as alkali roasting [111], [112]. Interestingly, K_2CO_3 also induced sintering in MAF, even though MAF is not subject to any separation of Fe-oxide to the surface (the particle consists of almost pure Fe already). Increased sintering due to enhanced Fe-migration in ilmenite might therefore be only a part of the explanation, and there might be something more happening related to the interaction between the Fe-oxide and K. It was not possible to determine a more detailed mechanism in this study, but the effect would be interesting to study further.

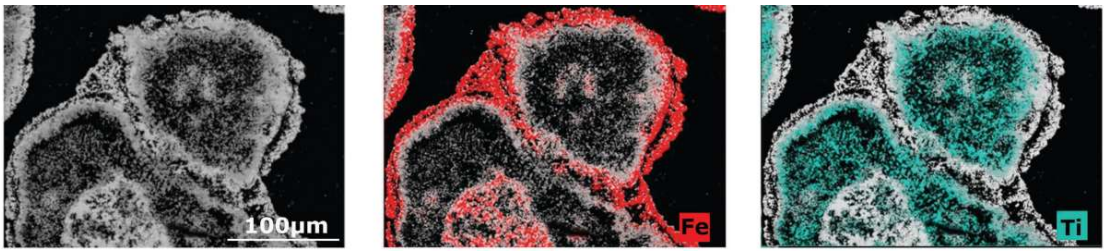

Figure 20: *Agglomerate of ilmenite form the fluidized bed experiment with addition of K_2CO_3. The particles are connected via the Fe-oxide layer on their surfaces. Very low K concentrations were observed in the sintered Fe-layer.*

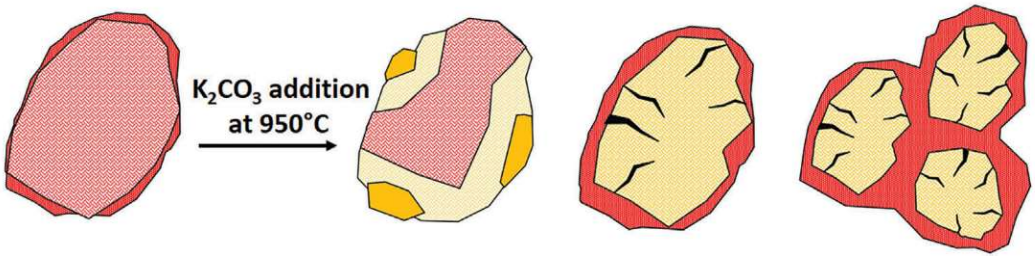

Figure 21: *The following mechanism is suggested for interaction between ilmenite and K_2CO_3: The inwards diffusion of K accelerates the migration of Fe to the surface of ilmenite particles, which increases the risk for solid state sintering.*

The fuel conversion, presented in Figure 22, was temporarily negatively affected by the addition of K_2CO_3. The correlation between fuel conversion and fluidization was not clear. It might have to do with a temporary coating of the particles by melt, but this intermediate step is not visible in the study as the particles were only studied after the end of the experiment. In previous studies, the addition of K to ilmenite has been related rather to increased fuel reactivity. A couple of different explanations have been suggested. Bao et al. [113] saw an increased reactivity of CO in fluidized experiments with K-impregnation of ilmenite and suggested that this was because the diffusion of K into the particle promoted pore formation in the material structure, and that the BET surface area, therefore, increased with K-concentration. Hildor et al. [82] found from fixed bed interactions that the reduction of ilmenite by CO was faster when K_2CO_3 was present. They suggested that the increased reduction rate was due to the enhanced iron migration taking place, and thus higher availability of Fe-oxide on the particle surface when ilmenite separated into K-titanate and Fe-oxide. However, in both referenced studies [82], [113], ilmenite was impregnated or premixed with the K_2CO_3 before the experiments, while in the current study, the ilmenite was activated in many reduction-oxidation cycles before the addition of K_2CO_3. The discrepancy between those and the current study regarding increased/decreased

reactivity might therefore be because K_2CO_3 is mainly involved in the activation of ilmenite, and not later in the continuous operation.

As compared to the pure Fe-oxide oxygen carriers Glödskal and MAF, the presence of Ti in the material greatly enhanced the K-absorption ability. This is highly relevant, as the combination of high K-capture and low agglomeration tendency is very beneficial for the application of high-alkali fuels.

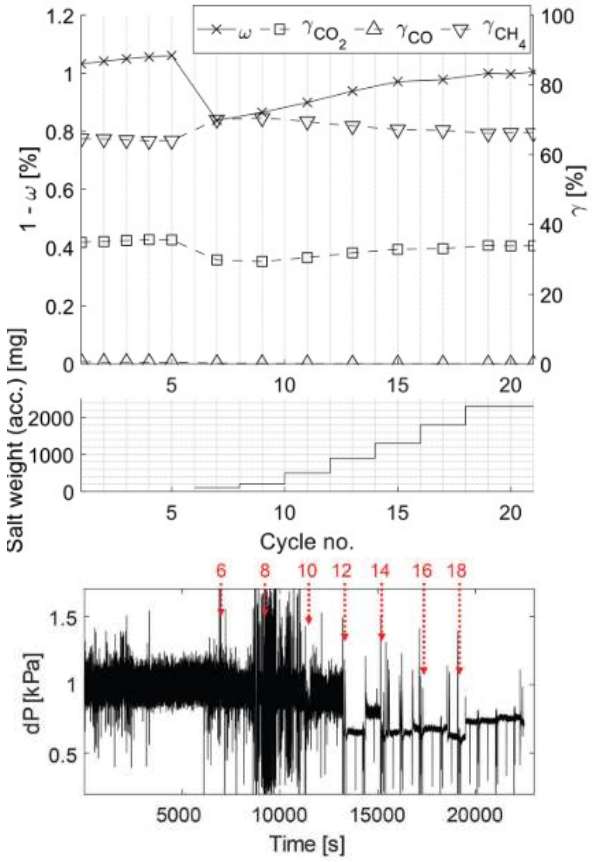

Figure 22: *Fuel conversion during the 950°C fluidized bed experiment with Ilmenite as oxygen carrier and addition of K_2CO_3. The K_2CO_3-addition starts at cycle 6, where a temporary decrease in fuel conversion is observed. ω_f is the mass-based conversion reached at the end of each reduction (100- ω_f is presented here). The parameters are explained in section 3.1.3.*

Figure 23: *The pressure drop recorded during the experiment. The sudden decrease in pressure drop and fluctuation amplitude at cycle 12 indicates defluidization.*

4.3. Interaction between K and the slag-based materials (copper smelter slag and LD-slag)

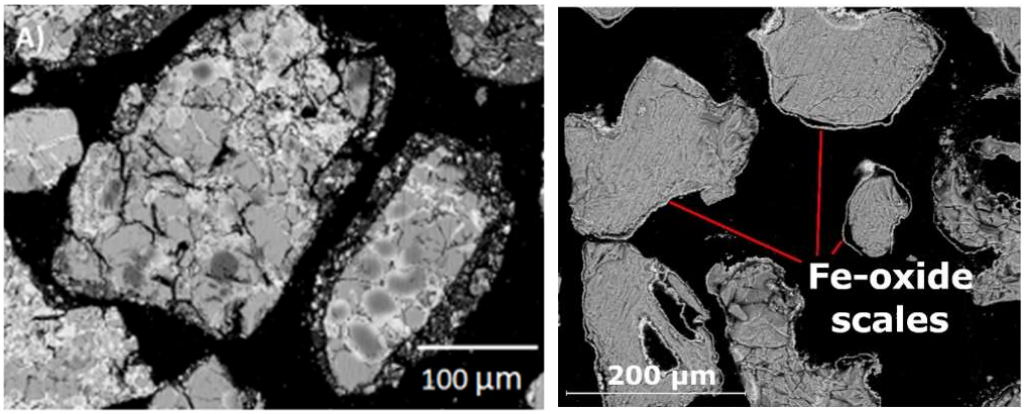

Figure 24: *Fresh LD-slag and Järnsand. SEM micrographs taken on the cross-section of some particles.*

Järnsand and LD-slag are discussed here together, but there are some considerable differences between the materials. They both contain mainly Fe, Si, Al, and Ca-oxides, as seen in Table 4. LD-slag also contains considerable amounts of Mg, Mn, and V. LD-slag is inhomogeneous, regarding the elemental distribution of its components, while Järnsand has a more homogeneous composition. SEM micrographs of both materials before experiments are presented in Figure 24. The following section provides results from the lab-scale experiments, while the analysis of Järnsand samples from the semi-industrial scale boiler will be discussed later in section 5.1.1.

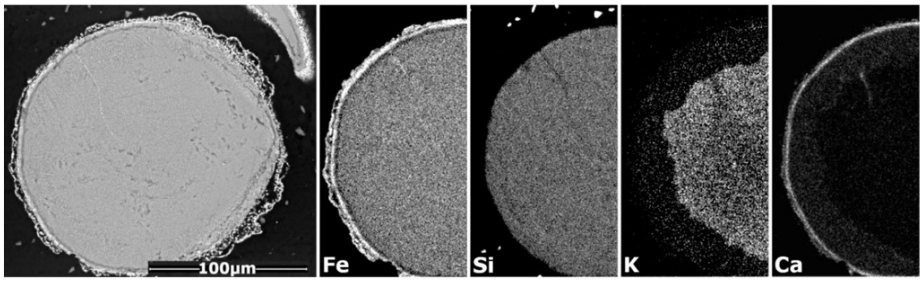

Figure 25: *Distribution of Fe, Si, K, and Ca in the cross-section of a Järnsand particle from a fluidized bed experiment with the addition of K_2CO_3 at 950°C. The K has migrated to the core of the particle, while Fe and Ca have formed a layer on the outside. The analysis is SEM-EDS.*

The interaction with K_2CO_3 in the fluidized bed reactor had no effect on the fuel conversion of Järnsand but resulted in agglomeration after a total addition of 240 or 910 mg at 850 or 950°C, respectively. K was transported to the interior of the particle, forming K-silicates, as seen in Figure 25. The XRD analysis failed to detect any crystalline K-phase, likely because the K-containing phase was amorphous or at too low concentrations. A migration of Ca towards the oxygen-rich surface was observed, a phenomenon that has been observed before in ilmenite samples [42].

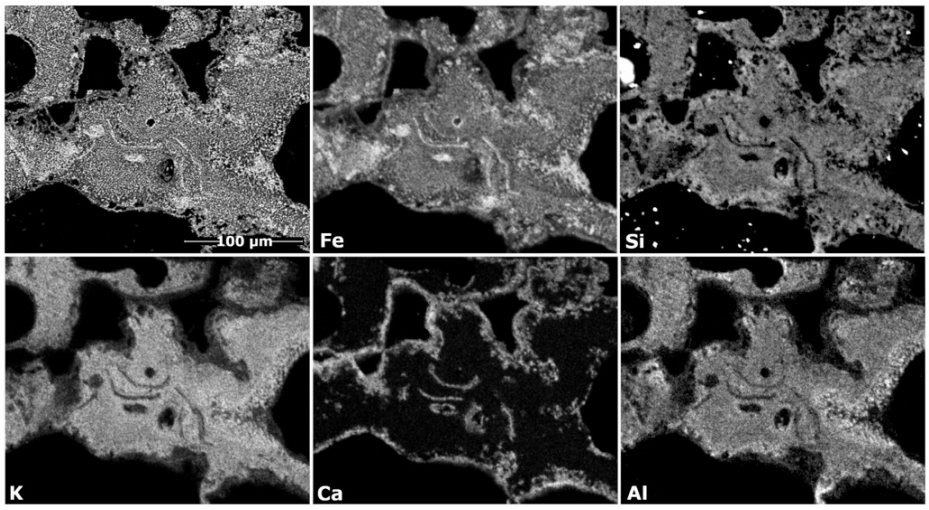

Figure 26: *Distribution of Fe, Si, K, Ca, and Al in the cross-section of agglomerated Järnsand from a fluidized bed experiment with the addition of K_2CO_3 at 950°C. K, Si, and Al overlap, and the particles look softened and deformed. The analysis is SEM.*

An increased amount of K resulted in the formation of agglomerates. At 950°C, the behaviour seen in Figure 26 was observed, where the morphology and shape of the material suggest that there has been melt formation and softening of the particles. At 850°C, no signs of a melt formation or softening of particles were observed, which was attributed to the presence of mainly Al and Mg in the material. In contrast, the melting temperature of "pure" K-silicate $K_2Si_4O_9$ is 770°C [76], and melt formation was therefore predicted at 850°C in the ternary Fe-Si-K diagram in Figure 17. When including the remaining components of the material in the calculations, the predicted melting temperature was increased to above 900°C. The predominant phases are presented in Figure 27, showing that below 900°C, K is bound in solid feldspar ($KAlSi_3O_8$) and low amounts of $K_2MgSi_5O_{12}$. Some agglomeration at 850°C was anyway observed, via a solid sintering mechanism like the one seen for ilmenite, MAF and Glödskal. Ca was not predicted to contribute to the capture of K in Järnsand, and no overlap between K and Ca was seen in the SEM-EDS analysis.

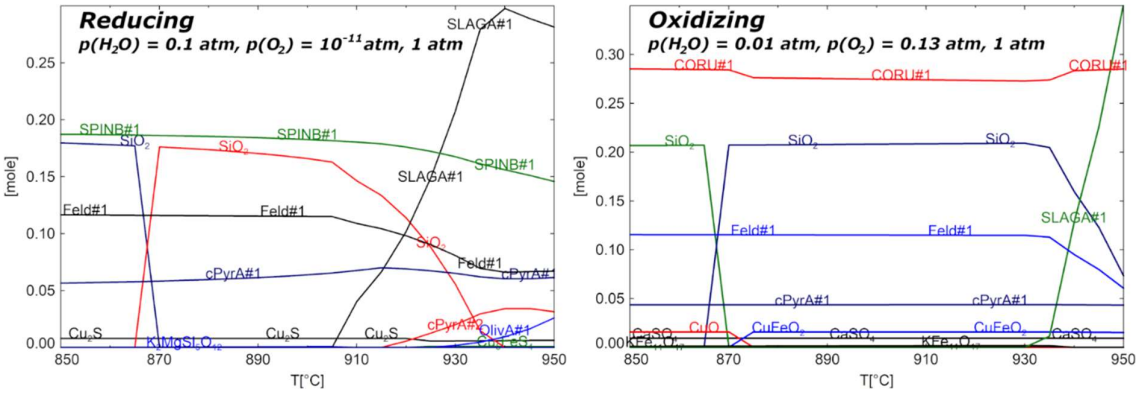

Figure 27: *Predicted predominant phases in Järnsand mixed with K_2CO_3, as a function of temperature. The slag phase (melting) is predicted to form at 900 and 930°C at reducing and oxidizing conditions, respectively. Fe is mainly in SPINB#1 (Fe_3O_4) and CORU#1 (Fe_2O_3). Feld#1 (feldspar) is mainly $KAlSi_3O_8$, cPyrA#1 (pyroxene) is on the form $XY(Si,Al)_2O_6$ containing varying amounts of mainly Mg, Ca, and Fe.*

For LD-slag, it was found in the TGA that the reactivity was negatively affected by K_2CO_3, showing no clear reduction and oxidation pattern. The contrast to LD-slag without K_2CO_3 is apparent in Figure 28. The reasons for the decreased reactivity were not apparent from the material analysis. The uptake of K in LD-slag was low but K was absorbed better in LD-slag than in pure Fe-oxide. Interestingly, the K did not mainly overlap with Si in the LD-slag, but with Ca. Further, no agglomeration was found in LD-slag mixed with K_2CO_3, based on the fixed bed experiment. Previous studies on LD-slag in OCAC operation [50], [51] concluded that it has a comparably low ability to absorb K. Due to this, high alkali levels in the gas phase affected the combustion negatively.

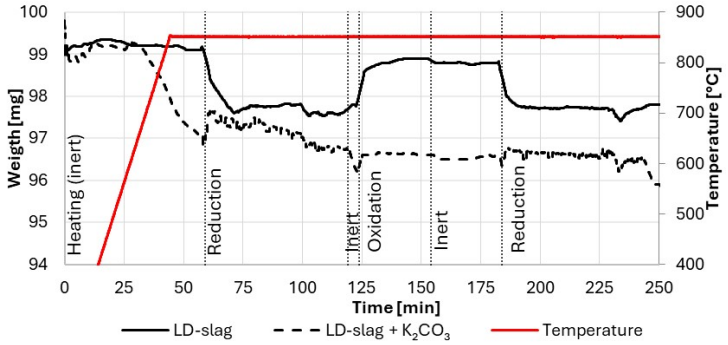

Figure 28: *Recorded weight change during the TGA with LD-slag and LD-slag mixed with K_2CO_3. Reduction is related to a decrease in weight, as the oxygen carrier contains less and less oxygen. Oxidation increases the weight of the oxygen carrier. The pure LD-slag follows this pattern, but the LD-slag mixed with K_2CO_3 doesn't.*

4.4. Interactions with KH_2PO_4

KH_2PO_4 decomposes into KPO_3 when heated. KPO_3 has a melting temperature of 807°C and sticks to particle surfaces, thus, the interaction with KH_2PO_4 happens under different conditions. However, even though melt formation was seen in all the studied oxygen carriers mixed with KH_2PO_4, the addition had different effects depending on the material.

In MAF and Glödskal, the interaction with KH_2PO_4 resulted in agglomeration. The particles were glued together by a phase with equal molar amounts of Fe, K, and P. This is seen in Figure 29, showing the SEM-EDS analysis of agglomerated Glödskal particles. In both MAF and Glödskal, very low concentrations of K were observed inside the particles. The reduction and oxidation of Glödskal, measured in TGA (Figure 30), was negatively affected by the addition of KH_2PO_4, probably because particles were partly coated by the melt which blocked the contact between the fuel and the oxygen carrier. A slight negative effect on fuel conversion was observed also for MAF when KH_2PO_4 was added to the fluidized bed.

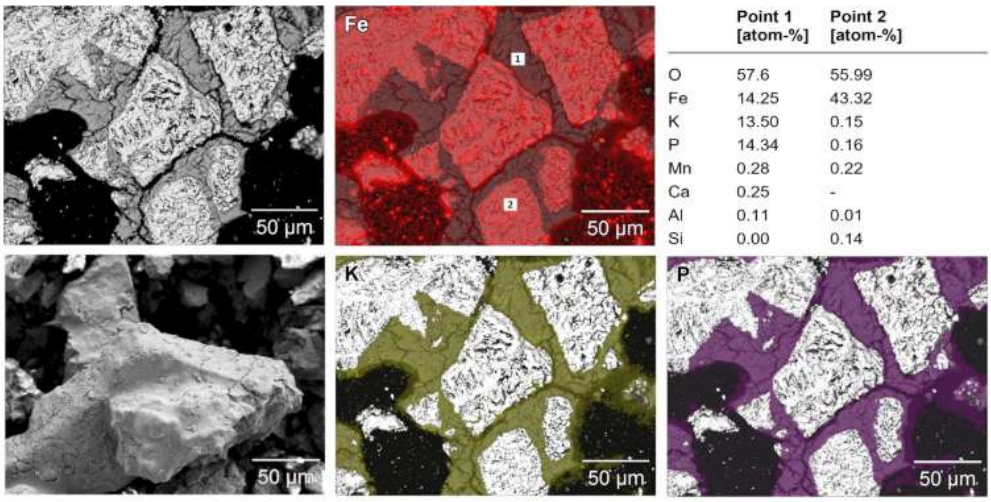

	Point 1 [atom-%]	Point 2 [atom-%]
O	57.6	55.99
Fe	14.25	43.32
K	13.50	0.15
P	14.34	0.16
Mn	0.28	0.22
Ca	0.25	-
Al	0.11	0.01
Si	0.00	0.14

Figure 29: *Agglomerate of Glödskal from the fixed bed experiment with KH_2PO_4-exposure. The glue between the particles is made of equal molar parts of Fe, K, and P. The table shows the concentration in the glue (point 1) and the particle (point 2).*

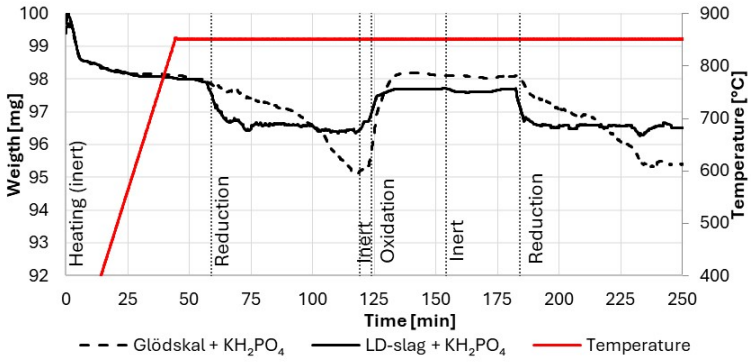

Figure 30: *Recorded weight change during the TGA with and Glödskal and LD-slag mixed with KH_2PO_4. Compared to the reference experiments presented in Figure 14 and Figure 28, LD-slag was not affected by the addition, but Glödskal had a much slower reduction when KH_2PO_4 was present.*

The interaction between ilmenite and KH_2PO_4 has not been studied in the current work, but a fixed bed experiment has been conducted previously by Hildor et al. [82]. They found that the reactivity was very negatively affected in TGA because KPO_3 melt covered the particles, and they also found that the glue phase between agglomerated particles has the same composition as seen with MAF and Glödskal. This phase was also observed in the fluidized bed experiments by Zevenhoven et al. under oxidizing conditions [81]. When the K exists as a P-K-melt, the inwards diffusion of K into the ilmenite particle does not take place.

With LD-slag and Järnsand, the interaction with KH_2PO_4 also resulted in the formation of agglomerates. Both Järnsand and LD-slag contain significant amounts of Ca, and Ca from the oxygen carrier migrated from the particles into the melt. This is seen in the SEM-EDS analysis presented in Figure 31 for LD-slag. The blue area is the phase formed by the interaction with KH_2PO_4, and it has the composition presented in the table. This changed the conditions for agglomeration, as the presence of Ca in the melt increased the melting temperature, making the coating layer less sticky. As a result, LD-slag particles were not coated by melt to the same extent, and the reduction, measured in the TGA, was not affected by the addition of KH_2PO_4. As compared to the Glödskal sample which was glued together into a slab and stuck in the sample holder, LD-slag was easier to remove, and the particles separated easily.

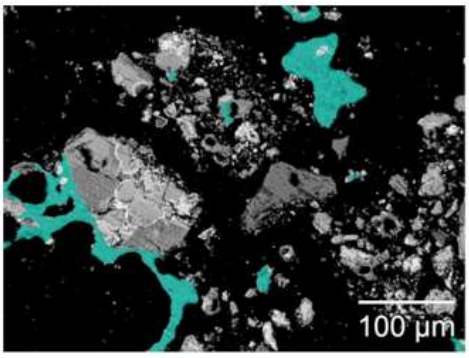

	Composition [atom-%]
O	25.39
K	25.62
P	23.75
Ca	20.40
Fe	2.40
Si	1.84
Mn	0.60

Figure 31: *LD-slag agglomerates formed by interaction with KH_2PO_4. The analysis is SEM-EDS on the cross-section. The composition of the area shaded in blue is presented in the table. A built-in phase-analysis function in the EDS analysis software was used to produce the blue map and composition.*

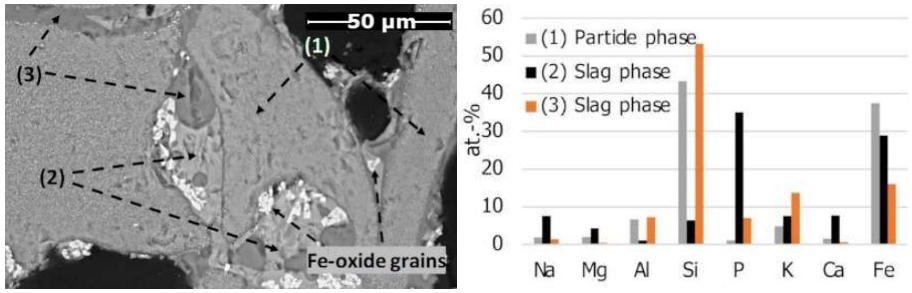

Figure 32: *Järnsand agglomerate formed by the interaction with KH_2PO_4. SEM-EDS analysis on the cross-section. Four different types of compositions are present: (1) The "particle phase" with a homogenous elemental distribution like fresh Järnsand. (2) Bridge/slag phase formed by the KH_2PO_4 interaction. Rich in mainly Fe and P. (3) Bridge/slag phase rich in Si and K. Low amounts of Al, Fe, and P are present. (4) Small grains of Fe-oxide located close to the particle surface.*

For Järnsand, the interaction with KH_2PO_4 involved both Fe and Ca, which partly migrated from the particles and were absorbed by the K-P-rich melt. The elemental compositions of different phases formed in the sample are presented in Figure 32. Interestingly, K and P mainly separated into two different phases, as seen from the analysis. Si, P, Ca and Fe were also present in the melt. The interaction with KH_2PO_4 resulted in the defluidization of the Järnsand bed and negatively affected fuel conversion.

The involvement of Ca in the presence of K and P and the formation of $CaKPO_4$, $Ca_{10}K(PO_4)_7$ and $Ca_5(PO_4)_3OH$ was discussed in section 2.3. The conclusions from the study with Järnsand and LD-slag are that the Ca inherent to the materials is involved in the ash chemistry in a similar way, which is likely positive for the reduced risk of agglomeration in the presence of K- and P-rich fuels.

5. Results Part II: Large-scale OCAC operation

An important aspect of the large-scale utilization of oxygen carriers is the availability of potential bed material and the procurement logistics. A lot of focus in this work has thus been on finding materials that are available in sufficient amounts. Using oxygen carriers that already exist as large material flows in the industry has some clear advantages when it comes to scaling up, at least in short-term. The production processes and properties of these materials are well known, and facilities for processing, transportation, etc. are already in place. Further, since the utilization degree of some of those materials is low, the cost could also be quite low. There are some materials with seemingly suitable properties that could be utilized more or less directly from the source.

As discussed in the background, the conversion of biomass- and waste-derived fuels is expected to be associated with high bed material consumption rates. Before discussing the use of novel bed materials, it is of interest to first understand the current situation with silica sand. Silica sand has a quite short lifetime in the boiler because it quickly becomes degenerated by ash interactions. The bed material consumption rates in kg/MW_{th} for some CBF and BFB biomass boilers are presented in Figure 33, showing that the consumption differs greatly between different plants. The operation with ilmenite in Örtofta and Eskilstuna is included for comparison.

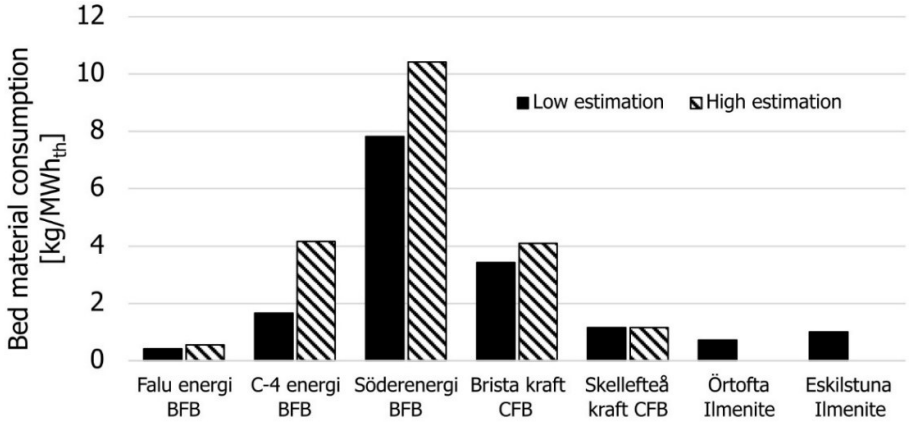

Figure 33: *Bed material consumption (kg/MWh$_{th}$) in seven biomass-fired boilers. The data for silica sand operation (Falu, C-4, Söderenergi, Brista and Skellefteå) is from Öhman et. al* [114]. *The data Örtofta (with ilmenite) is from Moldenhauer et al.* [40]. *The data for Eskilstuna is previously unpublished.*

By means of calculations and well-grounded assumptions, the size of total annual bed material consumption in Sweden was estimated to be 160-180 kton [5] (**Paper IV**). This was confirmed with Sibelco Nordic, which is the mineral trading company currently responsible for providing most of the silica sand to Swedish boilers (although the precise size of the market was not disclosed). The Swedish quartz sand production was between 579 and 783 kton between the years 2008 and 2018, according to the Geological Survey of Sweden [115]. Notably, this means that sand consumption in fluidized bed boilers corresponds to approximately 20% of the total Swedish quartz sand production. As silica sand is relatively cheap, a large consumption in the boiler can be employed to ensure a low risk of agglomeration and defluidization of the bed.

However, silica sand is a virgin resource and natural sand reserves play an important role in groundwater production. Protecting sand reserves is therefore part of Sweden's environmental goals [116]. Figure 33 shows a lower consumption of bed material when ilmenite was used. Further, previously unpublished data from an MSW-fired CFB unit in Händelö showed that when ilmenite was used as bed material, a bed consumption of 3 kg/MWh was possible. The consumption could be further decreased to 0.8 kg/MWh when a recycling system based on magnetic separation (explained in [47]) was introduced. This exemplifies that changing to a bed material with a different composition can significantly change the ash interactions, and thereby the required amount of material.

The tonnage cost of the bed material is crucial. Table 7 presents examples of known costs for processing small batches of bed material for semi-industrial scale experimental campaigns. In the examples, the cost of the raw materials was small in comparison to activities like calcination, drying, milling, sieving, etc. Tierga iron ore, given as an example, had a raw material cost of 310 €/ton, while the final cost was 6433 €/ton, and about 40% of the raw material was lost in the process. The yield can likely be increased with a fine-tuning of the process. Note that the numbers presented in Table 7 represent the production of one-of-a-kind very small batches (around 10 tons) and are not representative of a scaled-up production. For a scale-up, it is necessary that the processing costs are reduced significantly, and a reduction by one order of magnitude for processing should be possible for dedicated production chains. The examples anyway show that every extra step of processing is related to a significant cost increase, and this will be true also for production at scale.

***Table 7**: Costs for preparation of oxygen-carrier particles to be used in semi-industrial scale experimental OCAC campaigns*.

	Tierga (Iron Ore)	**Sibelco (Mn-Ore)**	**Elwaleed C (Mn-Ore)**
Raw material batch size (tons)	25	25	20
Raw material cost (€/ton)	310	850	200*
Preparations etc. (€/batch)	-	-	4300
Calcination (€/ton)	1900	(pre-calcined)	-
Drying (€/ton)	750	-	-
Crushing from large chunks (€/ton)	-	450	-
Milling, sieving, dedusting, packaging (€/ton)	900	962.5	1080
Declaration of analysis for waste disposal (€/batch)	-	350	350
Disposal of residues (€/ton residues)	-	280	300
Amount 100–400 µm particles received (tons)	15 (estimated)	12.1	8.2
Yield in production (%)	60 (estimated)	48.4	41
Final cost (€/batch)	96 500	60 525	33 790
Final cost (€/ton particles)**	6433	5002	4121

* Assumed representative price for low grade ore.

** Note that that these are costs for preparation of one large batch for experimental purposes. Economics of scale and learning curve are likely to reduce these costs significantly for a dedicated manufacturing process.

Since every processing step adds costs, available materials should ideally be usable with minimal effort. Two materials that potentially would require little in terms of processing were identified in this study: granulated copper smelter slag (Järnsand) and iron ore magnetite fines (MAF). The granulation process of Järnsand, which already is operated at scale in Sweden, produces particles in a size range reasonably close to what is desired to have in boilers. The

product is also relatively dry and doesn't require any extra calcination. On top of that, the production quantities are very large: Boliden produces around 250-270 kton of granulated slag annually, and that corresponds only to around 1/3 of the total slag production (most it is air-cooled, and air-cooled slag has limited utilization). Another advantage for Järnsand is that it is produced as a by-product, in contrast to for example ilmenite and other ores which are primary resources. Based on this, together with the findings presented in **Paper III** regarding the interactions with K, Järnsand was identified as a suitable material to study further.

MAF is an intermediate product by LKAB for the production of steel. MAF is also in the form of particles in the size range 0-2 mm, and even though it's not the main form of ore products, the production of MAF (and hematite fines) is huge. Thus, it would be conceivably to extract a flow in existing processes for use in combustion application. This is a reason for studying further the utilization of ores and ore products as oxygen carriers.

5.1. Copper smelter slag as bed material in a wood-fired CFB boiler

An experimental campaign investigating Järnsand as an oxygen carrier was carried out over two weeks, with a total of 9 full days of operation. The first day was a reference day with the silica sand B28, which is the standard bed material for this boiler. For the following four days, the boiler was operated with a mixture of Järnsand and B28. In the second week, the bed consisted of 100% Järnsand for four consecutive days. The general operability of Järnsand as bed material was good. No unexpected problems occurred during feeding to the boiler or continuous operation. No agglomeration in the material was observed during particle sampling or emptying of the boiler. Some bed material was lost during operation in the form of fly ash. Most of this loss was, however, attributed to the elutriation of fine particles existing already in the fresh material, and not to attrition of the particles. Thus, it was concluded that the material had sufficiently good mechanical integrity for use in boilers.

The oxygen-carrying effect of Järnsand was studied by reducing the air-to-fuel ratio in the boiler and monitoring the response in CO emissions. An example of such an experiment is illustrated in Figure 34. As expected, the O_2 concentrations in the flue gas decreased, and eventually, the CO emissions increased. The response to this instantaneous change in air-to-fuel ratio was slower with Järnsand present. This is the first sign that Järnsand acts as an oxygen buffer in the bed: initially, lowering the oxygen surplus results in a change in the oxidation state of the oxygen carrier, rather than only a change in the gaseous O_2 concentration.

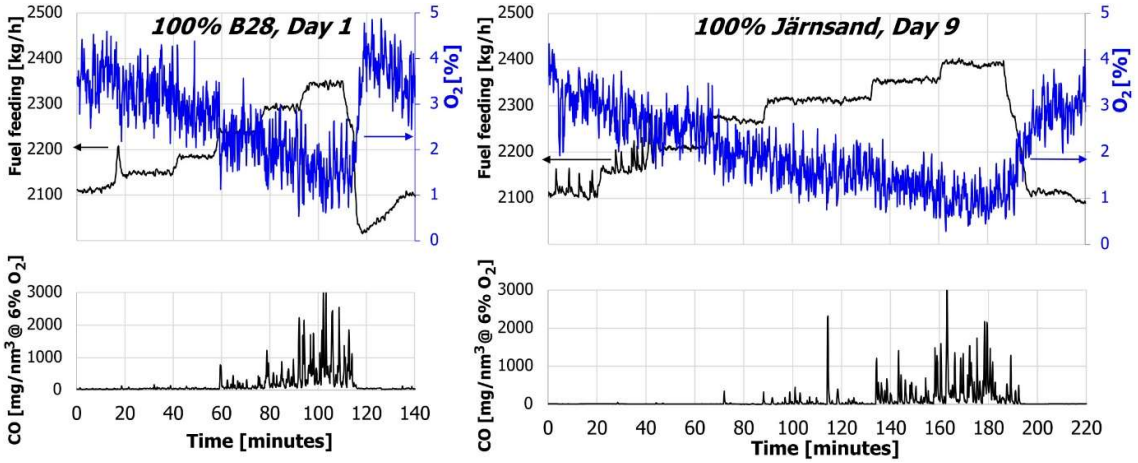

Figure 34: *Fuel flow [kg/h], O_2 concentration [%], and CO concentration [mg/nm^3 at 6% O_2]. Left: reference experiment with 100% B28 bed material, Day 1, right: last day of operation with 100% Järnsand, Day 9.*

The results for each day of experiments are presented in the graphs in Figure 35. The results are presented as CO concentrations in mg/nn^3 at 6% O_2 plotted against the air-to-fuel ratio, or the lambda value, which is the ratio between the airflow to the boiler and the stoichiometric air flow. The value is estimated according to Equation (7).

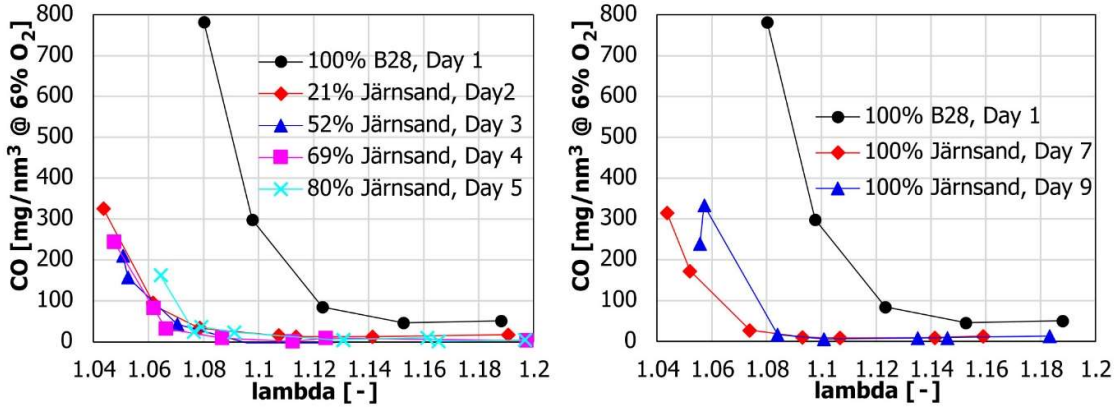

Figure 35: *The CO concentration in the flue gas as a function of the air-to-fuel ratio (lambda). The left graphs show the results from the first week with initially 100% B28 in the bed and mixtures of up to around 80% Järnsand in the bed (Day 1-5). The right graph shows the reference together with the 100% Järnsand days (Day 7 and Day 9). The CO concentrations are lower during the operation with Järnsand.*

$$\lambda = \frac{0.21}{0.21 - c_{O_2,dry}} \qquad \text{Equation (7)}$$

The following conclusions can be drawn from the operation at reduced air-to-fuel ratios:

- With Järnsand in the bed, the CO emissions were lower compared to the reference case. This was true for all lambda values, including the highest value which represents nominal operation (the lambda value is around 1.2).
- The bed with 21% Järnsand (Day 1) performed just as well as a 100% substituted bed (Day 7 and 9).

- With Järnsand in the bed, a lambda value of around 1.08 could be reached with essentially no increase in CO emissions. The same operation conditions with 100% B28 gave a 5 minutes-average CO concentration of about 800 mg/nm3 at 6% O2.
- With Järnsand in the bed, lambda values of around 1.06 were possible with a maximum mean CO concentration of only around 100-200 mg/nm3 on a 6% O2 basis. This lambda value corresponds to a flue gas oxygen concentration of 1.2%, measured in the dry gas.
- The NO emissions (not presented here but presented as a function of lambda in **Paper V**) decreased by approximately 30%. The mechanisms for NO formation in fluidized bed combustion and the effects of the oxygen carrier are not well understood and will not be discussed further here. It is anyway consistent with previous results that reducing the lambda value is in itself positive as it leads to lower NO emissions [50], [55].

The enhanced operation as compared to silica sand is likely an effect of the oxygen-carrying ability of Järnsand. The fuel conversion ability of Järnsand had already been confirmed in lab-scale experiments presented in **Paper III**, and the campaign demonstrated that this property had a positive effect on the conversion of solid fuel and that the bed material was active for at least 4 days in the boiler.

5.1.1. Bed material ageing

The CO concentrations were in general slightly higher during day 8 and day 9. This likely has to do with the ageing of the bed material in the boiler, during which the oxygen carrier absorbs alkali and other ash species. As discussed earlier, alkali accumulation affects the fuel burnout negatively. Indeed, the total elemental analysis of material samples, presented in Figure 36, showed that the K concentration increased in the bed material from day 6 to day 9, during which no fresh bed material was added. It should be noted, however, that even as K was accumulating in the bed during day 6 to day 9, the increase in CO emissions were not exceedingly high, and resembled "normal" levels, as is shown in **Paper V**.

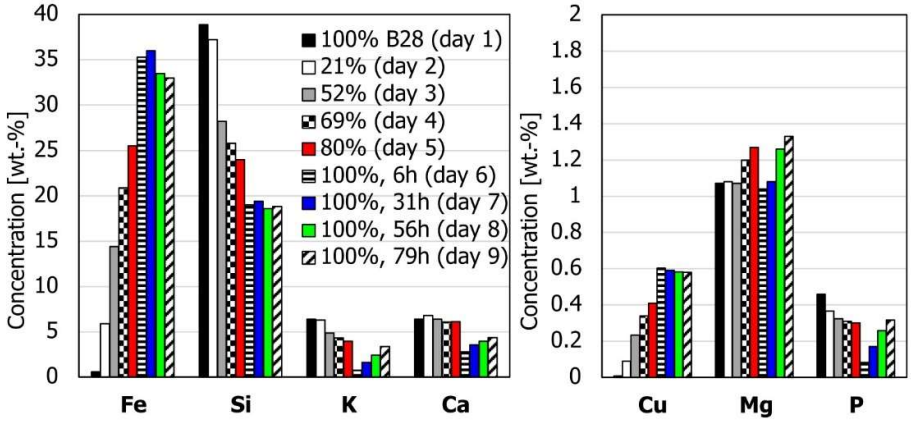

Figure 36: *Total elemental composition of bed material samples from the boiler. B28 and Järnsand mixtures (day 1-day 5) and operation with 100% Järnsand (day 6-day 9). Note that the scale on the y-axis for Cu, Mg, and P are different.*

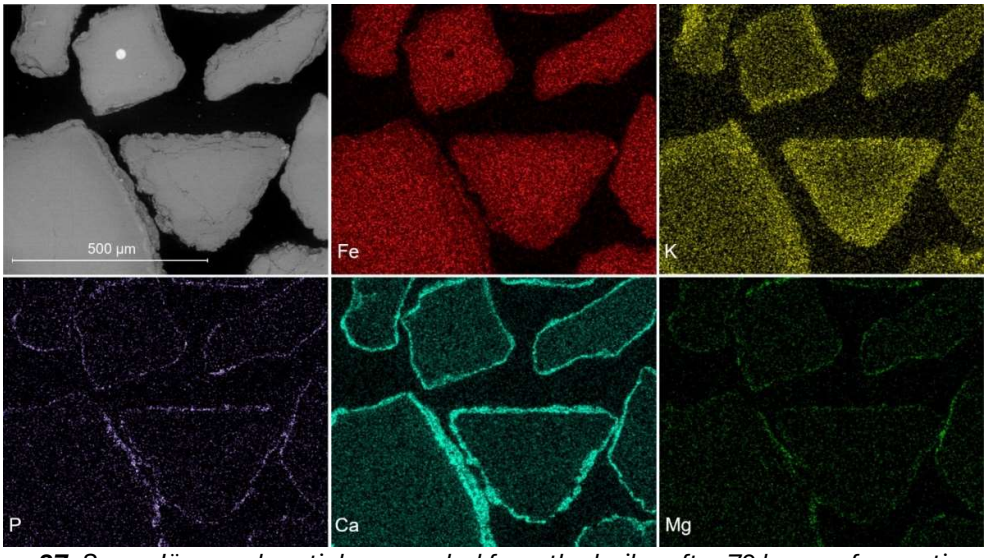

Figure 37: *Some Järnsand particles sampled from the boiler after 79 hours of operation. The analysis is SEM-EDS on the cross-section. K has been absorbed by the particles. There's a layer of mainly Ca, P, and Mg on the particle surface.*

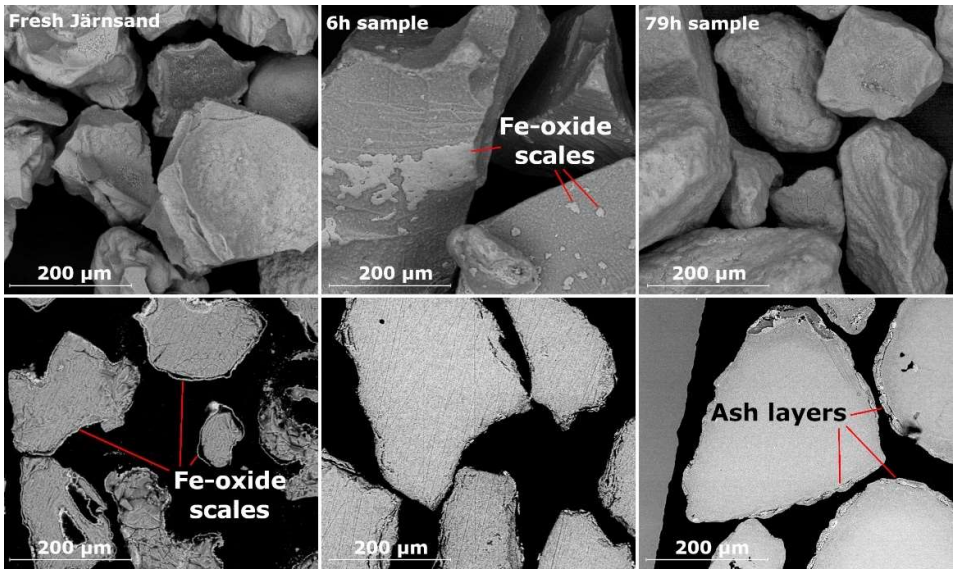

Figure 38: *SEM micrographs of (left) fresh Järnsand particles and Järnsand particles sampled from the boiler after (middle) 6 hours or (right) 79 hours of operation. The lower row is on the cross-section*

Bed material samples extracted from the boiler during the campaign were studied with SEM-EDS. The elemental distribution of Fe, K, P, Ca, and Mg are presented in Figure 37. The findings regarding the material ageing in the boiler are summarized here, along with some comparison with the samples from fluidized bed interaction experiments with K_2CO_3 addition:

- **K absorption and migration into the particle.** The K was evenly spread out across the whole cross-section of the particles. A bulk K-concentration of around 3.5wt.-% was observed for both the lab-scale sample and the boiler sample with the most time in the boiler. For the lab-scale sample, this corresponded to the total amount of K added during the experiment. In the boiler sample, the innermost part of the particles had a lower K-concentration than closer to the surface, suggesting that the material was not saturated.
- **Ca-layer.** A Ca-layer was formed on the particle surface. The aged boiler sample showed a thicker Ca-layer than the lab-scale sample, which is expected since (i) the particle has been in operation for longer, i.e. the Ca in Järnsand has had a longer time to migrate, and (ii) because of the Ca contribution from the fuel ash, which is not present in the lab-scale experiments. The outer layer also contains Mg and P from the fuel, further arguing for the deposition of ash. Although no fuel analysis was done in this work, the general ash composition of wood in Figure 5 displays high concentrations of CaO.
- **Fe-layer formation.** A pronounced Fe-oxide layer was observed on the samples from the lab-scale experiments. This was not seen on the aged boiler sample, rather, the Fe-oxide layer present on the fresh particles (seen in the left in Figure 38) was worn off after some time. On top of that, a very low BET surface area and a dense inner structure of the particles were observed for the boiler sample. Fe-availability for the gas phase is crucial for the oxygen-carrying mechanism of the particles, and in the worst case, the lack of Fe-layer and the ash deposition on the surface deactivates the material (this was

discussed in [42], and observed in fixed bed experiment with ilmenite and KH_2PO_4 in [82]).

- **Agglomeration.** Agglomeration (and defluidization) was observed during the lab-scale experiment, but not in the boiler sample. The agglomeration in the lab-scale experiment was related to either high local K-concentrations and the formation of molten K-Si-oxide (this was seen at 950°C) or sintering between the Fe-layers (this was mainly seen in 850°C). For boiler operation, neither of the two mechanisms is likely to be a problem, as (i) the K-addition will be more even across the bed than in the lab-scale experiments, where locally very high K-concentrations are likely to form with the current method of feeding solid salt particles (ii) the temperature doesn't typically exceed 900°C in the boiler (although local hotspots might be experienced) and (iii) the "clean" Fe-oxide layer that resulted in sintering in the lab scale samples is likely less pronounced in the boiler samples, because of higher attrition but also because of more ash depositing on the surface. On top of that, a sintering effect was seen for ilmenite on the lab scale, but no agglomeration has been observed in ilmenite from boiler samples in previous studies.

It was also investigated whether the fluidization and oxygen-carrying properties of the bed material were affected by the ageing in the boiler. 20 g of bed material sample was placed in the fluidized bed reactor presented in section 3.1.3, and the bed was fluidized alternatingly with air and fuel at 850°C, representing the conditions in the boiler. The results showed higher CO_2 yields with the aged sample, extracted after 79 hours in the boiler, compared to the samples extracted after 2 or 6 hours. This is in line with previous studies, showing that fresh oxygen carriers undergo activation and that the oxygen-carrying properties increase over time. This is often attributed to the increased availability of Fe-oxide, because of the development of Fe-layers or pores/cracks forming in the particles.

6. General discussion

6.1. Summary of potassium interactions

From the current, and previous, studies of experimental large-scale utilization of oxygen carriers, it seems clear that alkali absorption is required for a good overall performance in the boiler. For example, due to the documented low uptake of K in LD-slag and poor results with respect to emissions in previous OCAC campaigns [50], [51], it is not likely that LD-slag alone would be a suitable oxygen carrier for biomass or waste-derived combustion. However, such materials should not be excluded from further consideration and investigation, and it is conceivable that such bed materials could be combined with an additive for handling the K-content of the fuels. In the campaigns with LD-slag and manganese ore, addition of ammonium sulphate worked well to handle the gas-phase alkali [50], [50]. Other options include the addition of elemental sulphur, or cofiring with sulphur-rich fuel. After all, LD-slag is a sizable by-product in the industry and could potentially be a cheap alternative to other materials.

If other compounds are present in the oxygen carrier material than iron oxide, the absorption of K into iron oxide itself is low. If available, K is more likely to interact with Ti, forming K-titanate, or Si, Mg, and Al, forming K-silicate, feldspar, or similar compounds. The absorption of K in relatively pure iron-oxide particles (like Glödskal and MAF) is low, and the interaction with K weakens the particle structure. This is associated with an increase in the reactivity with fuel, but if the particle can't sustain adequate mechanical strength or absorb K, such materials are likely not a suitable option to use as oxygen carriers during biomass combustion. Further, Glödskal is not produced in very large quantities, and MAF is a primary product and not a by-product.

Combustion of P-rich fuels would benefit from using one of the Ca-rich bed materials (Järnsand or LD-slag) as the incorporation of Ca in the melt increases the melting temperature by forming Ca-K-P phases. The lack of Ca in ilmenite and iron oxide results in the formation of a Fe-K-P phase, which contributes more to the agglomeration of the material. The idea of Ca-addition to the combustion of these types of fuels is not new, but the current study gives a better understanding of how the migration of Ca from the bed materials could affect the ash interactions positively.

6.2. Experimental methods used in the studies

Studying oxygen carriers in different experimental setups is a way to understand the interactions better. By comparing the results, we can also better understand how well the lab-scale experiments simulate the boiler conditions. This work contributes therefore both to the knowledge about the ash interactions, and to the development and evaluation of the experimental methods.

There are some considerable differences between the conditions in the boiler and in the lab-scale fluidized bed reactor used in this work. For example, the superficial gas velocity was up to 3 m/s in the boiler, but around 0.1 m/s in the lab reactor. The alkali concentration might be locally very high in the lab reactor since alkali was added in the form of solid model compounds and at a very high rate. The lab reactor could therefore represent a type of worst-case situation which would not be representative of the whole cross-section of the boiler, but which could

anyway arise locally and have a large effect on the bed material. For example, there are stagnant zones in the bottom of the bed, where the air injection doesn't reach the bed well. A comparison between boiler samples of Järnsand and samples from the interaction with K_2CO_3 was presented in section 5.1.1. The K interactions in the boiler agreed with the lab-scale experiments. The same can be said about ilmenite when comparing the results from the K_2CO_3 interactions with previously published findings in boiler samples. Although it's difficult to generalize, this anyway indicates that using model compounds in this way could be a suitable first step in evaluating the suitability of new oxygen carriers.

Further, the fixed bed interactions should result in even more severe agglomeration than the fluidized bed interactions. In a fluidized bed, the agglomerates have the possibility to break when the particles move around and hit each other and the reactor walls. In a fixed bed, the agglomerates cannot break once they're formed. A clear difference between the materials could anyway be observed with this method, and an agreement between the fixed bed experiments with Glödskal and the fluidized bed experiments with MAF was seen.

To gain more knowledge, in a future study, the fluidized bed reactor could be used with a wider range of ash model compounds, either as mixtures or in sequence. For example, it's evident from the literature study and the current investigation that the presence of Ca affects the agglomeration with K- and P-rich fuels. Including Ca-compounds in future experiments could increase the knowledge about (i) how the fuel-Ca is involved in the ash interactions with the oxygen carriers, (ii) how the Ca in the oxygen carrier is involved and (iii) how to use Ca as an additive in an efficient way.

It should be noted that the experimental methods used in this work are qualitative rather than quantitative. The expected behavior of the ash model compounds was discussed in section 3.1.4, but their exact behavior is difficult to predict. To close the material balance and get a quantitative evaluation of, for example, the retention of K in the bed, measurements of gas-phase alkali would be required. Even then, there are error sources that might be difficult to address, such as alkali interaction with the reactor material and condensation downstream of the reactor. This has been discussed extensively by Andersson et al. [66], [117], in their work with developing an experimental method with injection of ash compounds in the form of aerosols.

6.3. The future for copper smelter slag

According to the work presented in this thesis, the following properties of Järnsand would make it a suitable oxygen carrier for wood-fired OCAC operation:

- **Ash chemistry.** K can be captured. The formation of low-melting K-silicate and agglomeration is not likely to be a problem because of the high contents of Al, Mg, and Ca, etc. A slag formation temperature of above 900°C was calculated for a mixture of Järnsand and K_2CO_3.
- **Fluidization properties.** Järnsand has similar mechanical properties as silica sand.
- **Particle integrity.** Not subject to excessive attrition
- **Fuel reactivity** in line with for example ilmenite. The fuel reactivity (the conversion of methane and syngas) increased slightly during ageing in the boiler for 4 days.

- **Large-scale production.** Water-granulated Järnsand is produced and available in large quantities. Some processing (crushing/milling and sieving) is required, but extensive efforts are likely not required, in contrast to, for example, air-cooled slags.

Some aspects of Järnsand could be potential challenges with utilization, and some aspects simply need to be studied further. Some ideas for further studies are presented here:

- **Long-term operation.** The lifetime in the boiler was not exceeded in the campaign, as no operational problems such as increasing CO emissions or agglomeration were observed. Probably, based on the findings, increasing CO emissions as a function of volatile alkali would be the first indication that the bed needs to be regenerated, but other potential lifetime limits might be attrition or agglomeration (although neither seems likely).
- **Ash disposal.** Preferably, ash from biomass combustion should be returned to the forest so as not to deplete the soil from nutrients. Alternative bottom ash utilization might include construction aggregate for roads. However, the high content of, for example, Cu in Järnsand limits the possibilities for utilizing the ash and from the boiler. Careful leaching and total elemental analysis should be conducted to understand the risks. Probably, because of this, Järnsand is at least initially best suited for combustion of MSW or other waste-derived fuels, where the concentrations of Cu and other potentially toxic species are expected to be high anyway.
- **MSW combustion** (or other waste-derived fuels) with Järnsand has not been studied yet. The wide ash profile of MSW might be challenging and is associated with possible ash interactions that have not been covered yet.
- **Magnetic separation.** Some initial, unpublished investigations showed that Järnsand develops magnetic properties in the boiler. This would be useful for the separation of oxygen carrier and ash and for recirculation of the bed material. Especially in MSW, there can be expected to be large ash particles, chunks of rock and glass, etc., and a successful separation method would be beneficial for the lifetime of the material.

As ilmenite has been successfully operated in several boilers, it has become a natural benchmark oxygen carrier for large-scale OCAC operation. The interactions with Järnsand and ilmenite have some interesting similarities, as both materials show uptake of K into the core. The formation of KTi_8O_{16} was determined for ilmenite by XRD, but no crystalline phase could be determined for K-silicate, probably because it's amorphous. When it comes to the overall function of the materials, Järnsand and ilmenite seem to have similar properties. They both show a similar development regarding the formation of Fe- and Ca layers on the particle surface, and they both capture K added with the fuel. Both also perform well as bed material in Chalmers research boiler.

In the lab-scale experiments with K_2CO_3, the agglomeration was more severe and caused defluidization at lower K-concentrations in Järnsand than in ilmenite. The agglomeration mechanism differed. For ilmenite, it was only found that the agglomeration was through sintering of the Fe-layers on the surface. Järnsand showed this behaviour as well, but also the formation of soft/molten K-silicate. Agglomeration was, however, not observed in boiler samples.

7. Conclusions

This thesis has investigated the opportunities for the large-scale utilization of oxygen carriers for the conversion of biomass and waste-derived fuels. The work presented aimed to: (i) deepen the understanding of potassium interactions with iron-based oxygen carriers, (ii) develop a new method for studying ash interaction with model ash compounds, and (iii) investigate oxygen-carrying materials that exist as available products and by-products in the metallurgical industries for this purpose.

These are the main contributions from this work:

- A new method was developed that allows for experiments in a lab-scale fluidized bed reactor, where the oxygen carriers are subject to reduction and oxidation while feeding ash model compounds in the form of solid salt particles. With this method, K interaction in a large-scale boiler, or during chemical-looping combustion, can be simulated. This is a useful tool for getting an initial understanding of K capture and risk for agglomeration before using a new bed material.
- The inclusion of K in Fe-oxide is low. However, the interaction results in changes in the particle structure, and pure Fe-oxide materials are subject to poor particle integrity in the presence of high-K fuels.
- Ilmenite and copper smelter slag can capture K without it necessarily resulting in agglomeration. This is attributed to the Ti-content in ilmenite and the Si-, Al-, Mg-, and Ca-contents in copper smelter slag. This is considered a positive trait for the combustion of difficult fuels with significant alkali content.
- The operability of copper smelter slag as an oxygen carrier in a wood-fired CFB boiler is good, and no practical problems was experienced during the two-week campaign. The air-to-fuel ratio could be reduced successfully from 1.2 to 1.08 without increasing the CO emissions. The material reached a K-concentration of 3.5 wt.-% after 4 consecutive days of operation in a wood-fired boiler, without signs of agglomeration. This agreed well with the findings from the experiment with ash model compounds.
- Copper smelter slag is an industrial by-product with limited utilization; thus, it is a suitable substitution for virgin materials (such as silica sand and ilmenite).
- Swedish metallurgical industries produce large flows of materials that could be suitable as oxygen-carrying bed material. Granulated copper smelter slag (Järnsand) and iron ore magnetite fines (MAF) are two such materials that exist in large quantities and likely don’t require extensive processing.

Furthermore, from a literature review regarding large-scale OCAC operation, it was concluded that changing to ilmenite has resulted in reduced air-to-fuel ratios and increased boiler loads in several commercial boilers. It is argued that implementing OCAC in boilers could have a positive economic and environmental impact on the Swedish energy production. Furthermore, it could act as an intermediate step between conventional combustion and CLC, thus could accelerate the implementation of large-scale carbon capture and storage.

8. References

[1] B. Leckner and F. Lind, "Combustion of municipal solid waste in fluidized bed or on grate – A comparison," *Waste Manag.*, vol. 109, pp. 94–108, 2020, doi: 10.1016/j.wasman.2020.04.050.

[2] J. D. Morris, S. S. Daood, S. Chilton, and W. Nimmo, "Mechanisms and mitigation of agglomeration during fluidized bed combustion of biomass: A review," *Fuel*, vol. 230, pp. 452–473, 2018, doi: 10.1016/j.fuel.2018.04.098.

[3] A.-L. Elled, L.-E. Åmand, and B.-M. Steenari, "Composition of agglomerates in fluidized bed reactors for thermochemical conversion of biomass and waste fuels Experimental data in comparison with predictions by a thermodynamic equilibrium model," *Fuel*, vol. 111, no. 1, pp. 696–708, 2013, doi: https://doi.org/10.1016/j.fuel.2013.03.018.

[4] D. Kunii and O. Levenspiel, *Fluidization Engineering*. Stoneham, MA: Butterworth-Heinemann, 2004. doi: 10.1016/s0147-6513(04)00151-4.

[5] F. Störner, F. Lind, and M. Rydén, "Oxygen Carrier Aided Combustion in Fluidized Bed Boilers in Sweden — Review and Future Outlook with Respect to Affordable Bed Materials," *Appl. Sci.*, vol. 11, no. 17, 2021, doi: https://doi.org/10.3390/app11177935.

[6] H. Thunman, F. Lind, C. Breitholtz, N. Berguerand, and M. Seemann, "Using an oxygen-carrier as bed material for combustion of biomass in a 12-MWth circulating fluidized-bed boiler," *Fuel*, vol. 113, pp. 300–309, 2013, doi: 10.1016/j.fuel.2013.05.073.

[7] M. Mandø, "Direct combustion of biomass," in *Biomass Combustion Science, Technology and Engineering*, Woodhead Publishing Limited, 2013, pp. 61–83. doi: 10.1533/9780857097439.2.61.

[8] M. Zevenhoven, P. Yrjas, and M. Hupa, *Handbook of Combustion, Chapter 14: Ash-Forming Matter and Ash-Related Problems*, vol. 4. Weinheim: Wiley-VCH, 2010.

[9] B. Leckner, "Developments in fluidized bed conversion of solid fuels," *Therm. Sci.*, vol. 20, pp. S1–S18, 2016, doi: 10.2298/TSCI150703135L.

[10] H. Ritchie and P. Rosado, "Energy Mix," OurWorldInData.org. Accessed: Oct. 12, 2024. [Online]. Available: https://ourworldindata.org/energy-mix

[11] A. Coppola and F. Scala, "Chemical Looping for Combustion of Solid Biomass: A Review," *Energy and Fuels*, 2021, doi: 10.1021/acs.energyfuels.1c02600.

[12] A. A. Khan, W. de Jong, P. J. Jansens, and H. Spliethoff, "Biomass combustion in fluidized bed boilers: Potential problems and remedies," *Fuel Process. Technol.*, vol. 90, no. 1, pp. 21–50, 2009, doi: 10.1016/j.fuproc.2008.07.012.

[13] S. Mayrhuber, F. Normann, D. Yilmaz, and H. Leion, "Effect of the oxygen carrier ilmenite on NOX formation in chemical-looping combustion," *Fuel Process. Technol.*, vol. 222, p. 106962, 2021, doi: 10.1016/j.fuproc.2021.106962.

[14] M. M. Hossain and H. I. de Lasa, "Chemical-looping combustion (CLC) for inherent CO2-separations - a review," *Chem. Eng. Sci.*, vol. 63, no. 18, pp. 4433–4451, 2008, doi: 10.1016/j.ces.2008.05.028.

[15] J. Adánez, A. Abad, F. Garcia-Labiano, P. Gayan, and L. F. De Diego, "Progress in chemical-looping combustion and reforming technologies," *Prog. Energy Combust. Sci.*, vol. 38, no. 2, pp. 215–282, 2012, doi: 10.1016/j.pecs.2011.09.001.

[16] A. Lyngfelt, A. Brink, Ø. Langørgen, T. Mattisson, M. Rydén, and C. Linderholm, "11,000 h of chemical-looping combustion operation—Where are we and where do we want to go?," *Int. J. Greenh. Gas Control*, vol. 88, pp. 38–56, 2019, doi: 10.1016/j.ijggc.2019.05.023.

[17] A. Lyngfelt and C. Linderholm, "Chemical-Looping Combustion of Solid Fuels - Status and Recent Progress," *Energy Procedia*, vol. 114, no. November 2016, pp. 371–386, 2017, doi: 10.1016/j.egypro.2017.03.1179.

[18] H. Gu, L. Shen, J. Xiao, S. Zhang, T. Song, and D. Chen, "Iron ore as oxygen carrier improved with potassium for chemical looping combustion of anthracite coal," *Combustion and Flame*, vol. 159, no. 7. pp. 2480–2490, 2012. doi: 10.1016/j.combustflame.2012.03.013.

[19] A. Lyngfelt, *Oxygen carriers for chemical-looping combustion*. Elsevier, 2015. doi: 10.1016/B978-0-85709-243-4.00011-2.

[20] V. Purnomo, D. Yilmaz, H. Leion, and T. Mattisson, "Study of defluidization of iron- and manganese-based oxygen carriers under highly reducing conditions in a lab-scale fluidized-bed batch reactor," *Fuel Process. Technol.*, vol. 219, p. 106874, 2021, doi: 10.1016/j.fuproc.2021.106874.

[21] P. Moldenhauer, M. Rydén, and A. Lyngfelt, "Testing of minerals and industrial by-products as oxygen carriers for chemical-looping combustion in a circulating fluidized-bed 300 W laboratory reactor," *Fuel*, vol. 93, pp. 351–363, 2012, doi: 10.1016/j.fuel.2011.11.009.

[22] V. Masson-Delmotte *et al.*, "Global warming of 1.5°C - An IPCC Special Report on the impacts of global warming of 1.5°C above pre-industrial levels and related global greenhouse gas emission pathways, in the context of strengthening the global response to the threat of climate change," 2018. doi: 10.1002/9780470996621.ch50.

[23] M. Bui *et al.*, "Carbon capture and storage (CCS): The way forward," *Energy Environ. Sci.*, vol. 11, no. 5, pp. 1062–1176, 2018, doi: 10.1039/c7ee02342a.

[24] W. K. Lewis and E. R. Gilliand, "Production of Pure Carbon Dioxode," 2665972, 1954

[25] M. Ishida, D. Zheng, and T. Akehata, "Evaluation of a chemical-looping-combustion power-generation system by graphic exergy analysis," *Energy*, vol. 12, no. 2, pp. 147–154, 1987, doi: 10.1016/0360-5442(87)90119-8.

[26] J. Adánez, A. Abad, T. Mendiara, P. Gayán, L. F. de Diego, and F. García-Labiano, "Chemical looping combustion of solid fuels," *Prog. Energy Combust. Sci.*, vol. 65, pp. 6–66, 2018, doi: 10.1016/j.pecs.2017.07.005.

[27] A. Lyngfelt and B. Leckner, "A 1000 MWth boiler for chemical-looping combustion of solid fuels – Discussion of design and costs," *Appl. Energy*, vol. 157, pp. 475–487, 2015, doi: 10.1016/j.apenergy.2015.04.057.

[28] A. Lyngfelt, D. Pallarès, C. Linderholm, F. Lind, H. Thunman, and B. Leckner, "Achieving Adequate Circulation in Chemical Looping Combustion–Design Proposal for a 200 MWth Chemical Looping Combustion Circulating Fluidized Bed Boiler," *Energy and Fuels*, vol. 36, pp. 9588–9615, 2022, doi: 10.1021/acs.energyfuels.1c03615.

[29] A. Lyngfelt, "Chemical-looping combustion of solid fuels - Status of development," *Appl. Energy*, vol. 113, pp. 1869–1873, 2014, doi: 10.1016/j.apenergy.2013.05.043.

[30] Z. Li and T. Lei, “能动系研究团队在化学链燃烧技术研究中取得重大进展,” Department of Energy and Power Engineering, Tsinghua university. Accessed: Jul. 25, 2024. [Online]. Available: https://www.te.tsinghua.edu.cn/info/1095/3291.htm

[31] N. E. L. Haugen *et al.*, “Building the world’s largest Chemical Looping Combustion (CLC) unit,” *Int. J. Greenh. Gas Control*, vol. 129, p. 103975, 2023, doi: 10.1016/j.ijggc.2023.103975.

[32] P. Ohlemüller, J. Ströhle, and B. Epple, “Chemical looping combustion of hard coal and torrefied biomass in a 1 MWth pilot plant,” *Int. J. Greenh. Gas Control*, vol. 65, pp. 149–159, 2017, doi: 10.1016/j.ijggc.2017.08.013.

[33] A. Nandy, C. Loha, S. Gu, P. Sarkar, M. K. Karmakar, and P. K. Chatterjee, “Present status and overview of Chemical Looping Combustion technology,” *Renew. Sustain. Energy Rev.*, vol. 59, pp. 597–619, 2016, doi: 10.1016/j.rser.2016.01.003.

[34] M. Keller, H. Leion, and T. Mattisson, “Mechanisms of Solid Fuel Conversion by Chemical Looping Combustion (CLC) using Manganese Ore: Catalytic Gasification by Potassium Compounds,” *Energy Technol.*, no. 1, pp. 273–282, 2013, doi: 10.1002/ente.201200052.

[35] H. Leion *et al.*, “Solid fuels in chemical-looping combustion using oxide scale and unprocessed iron ore as oxygen carriers,” *Fuel*, vol. 88, no. 10, pp. 1945–1954, 2009, doi: 10.1016/j.fuel.2009.03.033.

[36] T. Mattisson, A. Lyngfelt, and H. Leion, “Chemical-looping with oxygen uncoupling for combustion of solid fuels,” *Int. J. Greenh. Gas Control*, vol. 3, no. 1, pp. 11–19, 2009, doi: 10.1016/j.ijggc.2008.06.002.

[37] F. Lind, A. Corcoran, and H. Thunman, “Validation of the oxygen buffering ability of bed materials used for OCAC in a large scale CFB boiler,” *Powder Technol.*, vol. 316, pp. 462–468, 2017, doi: 10.1016/j.powtec.2016.12.048.

[38] X. Li, A. Lyngfelt, D. Pallarès, C. Linderholm, and T. Mattisson, “Investigation on the Performance of Volatile Distributors with Different Configurations under Different Fluidization Regimes,” *Energy and Fuels*, 2021, doi: 10.1021/acs.energyfuels.1c04159.

[39] F. Lind, A. Corcoran, B.-Å. Andersson, and H. Thunman, “12,000 hours of operation with oxygen-carriers in industrially relevant scale,” *VGB PowerTech*, vol. 7, pp. 1–6, 2017.

[40] P. Moldenhauer, A. Corcoran, H. Thunman, and F. Lind, “A Scale-Up Project for Operating a 115 MWth Biomass-Fired CFB boiler with Oxygen Carriers as Bed Material,” in *5th International Conference on Chemical-Looping*, Park City, Utah, USA, 2018.

[41] A. Corcoran, J. Marinkovic, F. Lind, H. Thunman, P. Knutsson, and M. Seemann, “Ash properties of ilmenite used as bed material for combustion of biomass in a circulating fluidized bed boiler,” *Energy and Fuels*, vol. 28, no. 12, pp. 7672–7679, 2014, doi: 10.1021/ef501810u.

[42] A. Corcoran, P. Knutsson, F. Lind, and H. Thunman, “Mechanism for Migration and Layer Growth of Biomass Ash on Ilmenite Used for Oxygen Carrier Aided Combustion,” *Energy and Fuels*, vol. 32, no. 8, pp. 8845–8856, 2018, doi: 10.1021/acs.energyfuels.8b01888.

[43] F. Lind and P. Knutsson, “Distribution of oxygen and carbon monoxide in the cross section of a circulating fluidized bed furnace during operating with inert and oxygen active bed materials,” in *Clearwater clean energy conference*, Florida, USA, 2019.

[44] A. Corcoran, F. Lind, H. Thunman, and P. Knutsson, “Leachability of potassium from ilmenite used as bed material during OCAC,” in *23rd International Conference on Fluidized Bed Conversion*, Seoul, South Korea, 2018.

[45] A. Corcoran, P. Knutsson, F. Lind, and H. Thunman, “Comparing the structural development of sand and rock ilmenite during long-term exposure in a biomass fired 12 MWth CFB-boiler,” *Fuel Process. Technol.*, vol. 171, no. June 2017, pp. 39–44, 2018, doi: 10.1016/j.fuproc.2017.11.004.

[46] M. Vigoureux, P. Knutsson, and F. Lind, “Sulfur Uptake during Oxygen-Carrier-Aided Combustion with Ilmenite,” *Energy and Fuels*, vol. 34, pp. 7735–7742, 2020, doi: 10.1021/acs.energyfuels.0c00420.

[47] A. Gyllén, P. Knutsson, F. Lind, and H. Thunman, “Magnetic separation of ilmenite used as oxygen carrier during combustion of biomass and the effect of ash layer buildup on its activity and mechanical strength,” *Fuel*, vol. 269, p. 117470, 2020, doi: 10.1016/j.fuel.2020.117470.

[48] T. Berdugo Vilches, F. Lind, M. Rydén, and H. Thunman, “Experience of more than 1000 h of operation with oxygen carriers and solid biomass at large scale,” *Appl. Energy*, vol. 190, pp. 1174–1183, 2017, doi: 10.1016/j.apenergy.2017.01.032.

[49] F. Lind, M. Israelsson, and H. Thunman, “Magnetic separation for the recirculation of oxygen active bed materials when combusting municipal solid waste in large scale CFB boilers,” in *Clearwater clean energy conference*, Florida, USA, 2018.

[50] M. Rydén, M. Hanning, and F. Lind, “Oxygen Carrier Aided Combustion (OCAC) of Wood Chips in a 12 MW th Circulating Fluidized Bed Boiler Using Steel Converter Slag as Bed Material,” *Appl. Sci.*, vol. 8, no. 12, 2018, doi: 10.3390/app8122657.

[51] F. Hildor, T. Mattisson, H. Leion, C. Linderholm, and M. Rydén, “Steel converter slag as an oxygen carrier in a 12 MW th CFB boiler – Ash interaction and material evolution,” *Int. J. Greenh. Gas Control*, vol. 88, no. June, pp. 321–331, 2019, doi: 10.1016/j.ijggc.2019.06.019.

[52] F. Hildor *et al.*, “LD slag as an oxygen carrier for combustion processes,” in *5th International Conference on Chemical Looping*, Park City, Utah, USA, 2018.

[53] S. Pissot, T. Berdugo Vilches, J. Maric, and M. Seemann, “Chemical looping gasification in a 2-4 MWth dual fluidized bed gasifier,” in *23rd International Conference on Fluidized Bed Conversion*, Seoul, South Korea, 2018.

[54] M. Hanning, A. Corcoran, F. Lind, and M. Rydén, “Biomass ash interactions with a manganese ore used as oxygen-carrying bed material in a 12 MWth CFB boiler,” *Biomass and Bioenergy*, vol. 119, pp. 179–190, 2018, doi: 10.1016/j.biombioe.2018.09.024.

[55] M. Rydén, M. Hanning, A. Corcoran, and F. Lind, “Oxygen Carrier Aided Combustion (OCAC) of Wood Chips in a Semi-Commercial Circulating Fluidized Bed Boiler Using Manganese Ore as Bed Material,” *Appl. Sci.*, vol. 6, no. 11, p. 347, 2016, doi: 10.3390/app6110347.

[56] K. Davidsson, “Slutrapport för projekt: Användning av restprodukter från gjuterier som bäddmaterial vid avfallsförbränning,” Borås, 2019.

[57] K. Davidsson, B. Andersson, H. Leion, M. Hedberg, and P. Karmhagen, “Foundry slag as bed material in fluidised-bed combustion of waste (Extended abstract),” in *Nordic Flame Days*, 2019.

[58] Jernkontoret, *Stålindustrin gör mer än stål, Handbok för restprodukter 2018*. 2018.

[59] Åbo Akademi, "Åbo Akademi University Chemical Fractionation Database." Accessed: Oct. 01, 2024. [Online]. Available: https://web.abo.fi/fak/tkf/ook/bransle/database.php

[60] A. Grimm, N. Skoglund, D. Boström, C. Boman, and M. Öhman, "Influence of Phosphorus on Alkali Distribution during Combustion of Logging Residues and Wheat Straw in a Bench-Scale Fluidized Bed," *Energy and Fuels*, vol. 26, pp. 3012–3023, 2012, doi: 10.1021/ef300275e.

[61] T. K. Hannl, N. Skoglund, J. Priščák, M. Öhman, and M. Kuba, "Bubbling fluidized bed co-combustion and co-gasification of sewage sludge with agricultural residues with a focus on the fate of phosphorus," *Fuel*, vol. 357, no. April 2023, 2024, doi: 10.1016/j.fuel.2023.129822.

[62] L. J. R. Nunes, J. C. O. Matias, and J. P. S. Catalão, "Biomass combustion systems: A review on the physical and chemical properties of the ashes," *Renew. Sustain. Energy Rev.*, vol. 53, pp. 235–242, 2016, doi: 10.1016/j.rser.2015.08.053.

[63] P. Piotrowska *et al.*, "Fate of alkali metals and phosphorus of rapeseed cake in circulating fluidized bed boiler part 1: Cocombustion with wood," *Energy and Fuels*, vol. 24, no. 1, pp. 333–345, 2010, doi: 10.1021/ef900822u.

[64] T. Leffler, C. Brackmann, M. Berg, M. Aldén, and Z. Li, "Online Alkali Measurement during Oxy-fuel Combustion," *Energy Procedia*, vol. 120, pp. 365–372, 2017, doi: 10.1016/j.egypro.2017.07.217.

[65] I. Gogolev, A. H. Soleimanisalim, D. Mei, and A. Lyngfelt, "Effects of Temperature, Operation Mode, and Steam Concentration on Alkali Release in Chemical Looping Conversion of Biomass - Experimental Investigation in a 10 kWth Pilot," *Energy and Fuels*, vol. 36, pp. 9551–9570, 2022, doi: 10.1021/acs.energyfuels.1c04353.

[66] V. Andersson, Y. Ge, X. Kong, and J. B. C. Pettersson, "A Novel Method for On-Line Characterization of Alkali Release and Thermal Stability of Materials Used in Thermochemical Conversion Processes," *Energies*, vol. 15, no. 12, 2022, doi: 10.3390/en15124365.

[67] T. Berdugo Vilches, W. Weng, P. Glarborg, Z. Li, H. Thunman, and M. Seemann, "Shedding light on the governing mechanisms for insufficient CO and H2 burnout in the presence of potassium, chlorine and sulfur," *Fuel*, vol. 273, p. 117762, 2020, doi: 10.1016/j.fuel.2020.117762.

[68] V. I. Babushok, G. T. Linteris, P. Hoorelbeke, D. Roosendans, and K. van Wingerden, "Flame Inhibition by Potassium-Containing Compounds," *Combust. Sci. Technol.*, vol. 189, no. 12, pp. 2039–2055, 2017, doi: 10.1080/00102202.2017.1347162.

[69] M. Kuba, N. Skoglund, M. Öhman, and H. Hofbauer, "A review on bed material particle layer formation and its positive influence on the performance of thermo-chemical biomass conversion in fluidized beds," *Fuel*, vol. 291, p. 120214, 2021, doi: 10.1016/j.fuel.2021.120214.

[70] I. Staničić, T. Mattisson, R. Backman, Y. Cao, and M. Rydén, "Oxygen carrier aided combustion (OCAC) of two waste fuels - Experimental and theoretical study of the interaction between ilmenite and zinc, copper and lead," *Biomass and Bioenergy*, vol. 148, no. April, 2021, doi: 10.1016/j.biombioe.2021.106060.

[71] M. Zevenhoven-Onderwater, M. Öhman, B. J. Skrifvars, R. Backman, A. Nordin, and M.

Hupa, “Bed agglomeration characteristics of wood-derived fuels in FBC,” *Energy and Fuels*, vol. 20, no. 2, pp. 818–824, 2006, doi: 10.1021/ef050349d.

[72] C. Sevonius, P. Yrjas, and M. Hupa, “Defluidization of a quartz bed - Laboratory experiments with potassium salts,” *Fuel*, vol. 127, pp. 161–168, 2014, doi: 10.1016/j.fuel.2013.10.047.

[73] V. Barišić, L. E. Åmand, and E. Coda Zabetta, “The role of limestone in preventing agglomeration and slagging during CFB combustion of high phosphorus fuels,” in *World Bioenergy*, Jönköping, Sweden, 2008, pp. 1–6. [Online]. Available: http://fwcparts.com/publications/tech_papers/files/TP_CFB_08_03.pdf

[74] E. Brus, M. Öhman, and A. Nordin, “Mechanisms of bed agglomeration during fluidized-bed combustion of biomass fuels,” *Energy and Fuels*, vol. 19, no. 3, pp. 825–832, 2005, doi: 10.1021/ef0400868.

[75] H. He, D. Boström, and M. Öhman, “Time dependence of bed particle layer formation in fluidized quartz bed combustion of wood-derived fuels,” *Energy and Fuels*, vol. 28, no. 6, pp. 3841–3848, 2014, doi: 10.1021/ef500386k.

[76] R. Faust, T. B. Vilches, P. Malmberg, M. Seemann, and P. Knutsson, “Comparison of Ash Layer Formation Mechanisms on Si-Containing Bed Material during Dual Fluidized Bed Gasi fi cation of Woody Biomass,” *Energy and Fuels*, vol. 34, no. 7, pp. 8340–8352, 2020, doi: 10.1021/acs.energyfuels.0c00509.

[77] M. Bozaghian Bäckman, A. Rebbling, M. Kuba, S. H. Larsson, and N. Skoglund, “Bed material performance of quartz, natural K-feldspar, and olivine in bubbling fluidized bed combustion of barley straw,” *Fuel*, vol. 364, p. 130788, 2024, doi: 10.1016/j.fuel.2023.130788.

[78] E. Lindström, M. Sandström, D. Boström, and M. Öhman, “Slagging Characteristics during Combustion of Cereal Grains Rich in Phosphorus,” *Energy and Fuels*, vol. 21, no. 2, pp. 710–717, 2007, doi: 10.1021/ef060429x.

[79] D. Boström *et al.*, “Ash transformation chemistry during combustion of biomass,” *Energy and Fuels*, vol. 26, no. 1, pp. 85–93, 2012, doi: 10.1021/ef201205b.

[80] I. Staničić, J. Brorsson, A. Hellman, T. Mattisson, and R. Backman, “Thermodynamic Analysis on the Fate of Ash Elements in Chemical Looping Combustion of Solid Fuels–Iron-Based Oxygen Carriers,” *Energy and Fuels*, vol. 36, no. 17, pp. 9648–9659, 2022, doi: 10.1021/acs.energyfuels.2c01578.

[81] M. Zevenhoven *et al.*, “Defluidization of the oxygen carrier ilmenite – Laboratory experiments with potassium salts,” *Energy*, vol. 148, pp. 930–940, 2018, doi: 10.1016/j.energy.2018.01.184.

[82] F. Hildor, M. Zevenhoven, A. Brink, L. Hupa, and H. Leion, “Understanding the Interaction of Potassium Salts with an Ilmenite Oxygen Carrier Under Dry and Wet Conditions,” *ACS Omega*, vol. 5, no. 36, pp. 22966–22977, 2020, doi: 10.1021/acsomega.0c02538.

[83] I. Staničić, M. Hanning, R. Deniz, T. Mattisson, R. Backman, and H. Leion, “Interaction of oxygen carriers with common biomass ash components,” *Fuel Processing Technology*, vol. 200. 2020. doi: 10.1016/j.fuproc.2019.106313.

[84] D. Yilmaz and H. Leion, “Interaction of Iron Oxygen Carriers and Alkaline Salts Present in Biomass-Derived Ash,” *Energy and Fuels*, vol. 34, no. 9, pp. 11143–11153, 2020, doi: 10.1021/acs.energyfuels.0c02109.

[85] F. Störner, F. Hildor, H. Leion, M. Zevenhoven, L. Hupa, and M. Rydén, “Potassium Ash Interactions with Oxygen Carriers Steel Converter Slag and Iron Mill Scale in Chemical-Looping Combustion of Biomass - Experimental Evaluation Using Model Compounds,” *Energy and Fuels*, vol. 34, no. 2, pp. 2304–2314, 2020, doi: 10.1021/acs.energyfuels.9b03616.

[86] V. Purnomo, F. Hildor, P. Knutsson, and H. Leion, “Interactions between potassium ashes and oxygen carriers based on natural and waste materials at different initial oxidation states,” *Greenh. Gases Sci. Technol.*, 2023, doi: 10.1002/ghg.2208.

[87] F. Hildor, D. Yilmaz, and H. Leion, “Interaction behavior of sand-diluted and mixed Fe-based oxygen carriers with potassium salts,” *Fuel*, vol. 339, no. December 2022, p. 127372, 2023, doi: 10.1016/j.fuel.2022.127372.

[88] L. Chen, P. Li, and T. Song, “Biomass ash chemistry in chemical looping combustion: Interaction mechanism of potassium-ash and iron-based oxygen carriers,” *Biomass and Bioenergy*, vol. 183, p. 107154, 2024, doi: 10.1016/j.biombioe.2024.107154.

[89] V. Andersson, X. Kong, H. Leion, T. Mattisson, and J. B. C. Pettersson, “Gaseous alkali interactions with ilmenite, manganese oxide and calcium manganite under chemical looping combustion conditions,” *Fuel Process. Technol.*, vol. 254, no. February, p. 108029, 2024, doi: 10.1016/j.fuproc.2023.108029.

[90] D. Y. Lu, Y. Tan, M. A. Duchesne, and D. McCalden, “Potassium Capture by Ilmenite Ore as the Bed Material During Fluidized Bed Conversion,” *Fuel*, vol. 335, p. 127008, 2023, doi: 10.2139/ssrn.4232829.

[91] F. Störner, P. Knutsson, H. Leion, T. Mattisson, and M. Rydén, “An improved method for feeding ash model compounds to a bubbling fluidized bed – CLC experiments with ilmenite, methane, and K2CO3,” *Greenh. Gases Sci. Technol.*, vol. 13, no. 4, pp. 546–564, 2023, doi: 10.1002/ghg.2218.

[92] Z. Xu *et al.*, “High-temperature potassium capture by ilmenite ore residue,” *Proc. Combust. Inst.*, vol. 40, no. 1–4, p. 105531, 2024, doi: 10.1016/j.proci.2024.105531.

[93] V. Purnomo, I. Staničić, T. Mattisson, M. Rydén, and H. Leion, “Performance of iron sand as an oxygen carrier at high reduction degrees and its potential use for chemical looping gasification,” *Fuel*, vol. 339, p. 127310, 2023, doi: 10.1016/j.fuel.2022.127310.

[94] V. Purnomo, M. D. B. Takehara, R. Faust, L. A. Ejjesta, and H. Leion, “New approach for particle size and shape analysis of iron-based oxygen carriers at multiple oxidation states,” *Particulogy*, p. 106972, 2023, doi: 10.1016/j.partic.2024.01.010.

[95] H. Leion, A. Lyngfelt, M. Johansson, E. Jerndal, and T. Mattisson, “The use of ilmenite as an oxygen carrier in chemical-looping combustion,” *Chem. Eng. Res. Des.*, vol. 86, no. 9, pp. 1017–1026, 2008, doi: 10.1016/j.cherd.2008.03.019.

[96] H. Leion, T. Mattisson, and A. Lyngfelt, “Solid fuels in chemical-looping combustion,” *Int. J. Greenh. Gas Control*, vol. 2, no. 2, pp. 180–193, 2008, doi: 10.1016/S1750-5836(07)00117-X.

[97] P. Wang, H. Leion, and H. Yang, “Oxygen-Carrier-Aided Combustion in a Bench-Scale Fluidized Bed,” *Energy and Fuels*, vol. 31, no. 6, pp. 6463–6471, 2017, doi: 10.1021/acs.energyfuels.7b00197.

[98] M. Keller, H. Leion, T. Mattisson, and H. Thunman, “Investigation of natural and synthetic bed materials for their utilization in chemical looping reforming for tar elimination in

biomass-derived gasification gas," *Energy and Fuels*, vol. 28, no. 6, pp. 3833–3840, 2014, doi: 10.1021/ef500369c.

[99] P. Moldenhauer, C. Linderholm, M. Rydén, and A. Lyngfelt, "Avoiding CO2 capture effort and cost for negative CO2 emissions using industrial waste in chemical-looping combustion/gasification of biomass," *Mitig. Adapt. Strateg. Glob. Chang.*, 2019, doi: 10.1007/s11027-019-9843-2.

[100] H. Leion, T. Mattisson, and A. Lyngfelt, "Use of Ores and Industrial Products As Oxygen Carriers in Chemical-Looping Combustion," *Energy and Fuels*, vol. 23, pp. 2307–2315, 2009, doi: 10.1021/ef8008629.

[101] H. Leion, V. Frick, and F. Hildor, "Experimental method and setup for laboratory fluidized bed reactor testing," *Energies*, vol. 11, no. 10, 2018, doi: 10.3390/en11102505.

[102] R. L. Lehman, J. S. Gentry, and N. G. Glumac, "Thermal stability of potassium carbonate near its melting point," *Thermochim. Acta*, vol. 316, no. 1, pp. 1–9, 1998, doi: https://doi.org/10.1016/S0040-6031(98)00289-5.

[103] J. N. Knudsen, P. A. Jensen, and K. Dam-Johansen, "Transformation and release to the gas phase of Cl, K, and S during combustion of annual biomass," *Energy and Fuels*, vol. 18, no. 5, pp. 1385–1399, 2004, doi: 10.1021/ef049944q.

[104] T. Blomberg, "Which are the right test conditions for the simulation of high temperature alkali corrosion in biomass combustion?," *Mater. Corros.*, vol. 57, no. 2, pp. 170–175, 2006, doi: 10.1002/maco.200503905.

[105] H. B. Zhao, W. T. Xu, Q. Song, J. K. Zhuo, and Q. Yao, "Effect of Steam and SiO2 on the Release and Transformation of K2CO3 and KCl during Biomass Thermal Conversion," *Energy and Fuels*, vol. 32, no. 9, pp. 9633–9639, 2018, doi: 10.1021/acs.energyfuels.8b02269.

[106] C. W. Bale *et al.*, "FactSage thermochemical software and databases, 2010-2016," *CALPHAD Comput. Coupling Phase Diagrams Thermochem.*, vol. 54, pp. 35–53, 2016, doi: 10.1016/j.calphad.2016.05.002.

[107] R. Faust *et al.*, "Thermodynamic Modeling and Experimental Investigation of the System Fe–Ti–O-K for Ilmenite Used as Fluidized Bed Oxygen Carrier," *Energy and Fuels*, vol. in press, 2024, doi: 10.1021/acs.energyfuels.4c02016.

[108] H. Gu *et al.*, "Interaction between biomass ash and iron ore oxygen carrier during chemical looping combustion," *Chem. Eng. J.*, vol. 277, pp. 70–78, 2015, doi: 10.1016/j.cej.2015.04.105.

[109] J. Adánez, A. Cuadrat, A. Abad, P. Gayán, L. F. D. Diego, and F. García-Labiano, "Ilmenite activation during consecutive redox cycles in chemical-looping combustion," *Energy and Fuels*, vol. 24, no. 2, pp. 1402–1413, 2010, doi: 10.1021/ef900856d.

[110] A. Cuadrat, A. Abad, J. Adánez, L. F. De Diego, F. García-Labiano, and P. Gayán, "Behavior of ilmenite as oxygen carrier in chemical-looping combustion," *Fuel Process. Technol.*, vol. 94, no. 1, pp. 101–112, 2012, doi: 10.1016/j.fuproc.2011.10.020.

[111] S. Sanchez-Segado, A. Lahiri, and A. Jha, "Alkali roasting of bomar ilmenite: Rare earths recovery and physico-chemical changes," *Open Chem.*, vol. 13, no. 1, pp. 270–278, 2015, doi: 10.1515/chem-2015-0033.

[112] S. Z. El-Tawil, I. M. Morsi, A. Yehia, and A. A. Francis, "Alkali reductive roasting of ilmenite

ore," *Can. Metall. Q.*, vol. 35, no. 1, pp. 31–37, 1996, doi: 10.1179/cmq.1996.35.1.31.

[113] J. Bao, Z. Li, and N. Cai, "Promoting the reduction reactivity of ilmenite by introducing foreign ions in chemical looping combustion," *Ind. Eng. Chem. Res.*, vol. 52, no. 18, pp. 6119–6128, 2013, doi: 10.1021/ie400237p.

[114] M. Öhman, A. Nordin, E. Brus, B.-J. Skrifvars, and R. Backman, "Förbrukning av bäddmaterial i biobränsleeldade fluidbäddar p g a bäddagglomereringsrisk – beläggningsbildning och möjligheter till regenerering," 2001.

[115] Geological Survey of Sweden, "Bergverksstatistik 2018: Statistics of the Swedish Mining Industry 2018," 2019.

[116] Naturvårdsverket, "Sveriges Miljömål - Grundvatten av god kvalitet." Accessed: Feb. 09, 2021. [Online]. Available: https://www.sverigesmiljomal.se/miljomalen/grundvatten-av-god-kvalitet/grusanvandning/

[117] V. Andersson *et al.*, "Alkali-wall interactions in a laboratory-scale reactor for chemical looping combustion studies," *Fuel Process. Technol.*, vol. 217, no. December 2020, p. 106828, 2021, doi: 10.1016/j.fuproc.2021.106828.